

Radical-Pair Based Magnetoreception Amplified by Radical Scavenging: Resilience to Spin Relaxation

Daniel R. Kattnig*

University of Exeter, Living Systems Institute and Department of Physics, Stocker Road, Exeter, Devon, EX4 4QD, United Kingdom

* Author for correspondence: d.r.kattnig@exeter.ac.uk, tel: +44 (0) 1392 72 7479

Abstract

Birds and several other species are equipped with the remarkable ability to sense the geomagnetic field for the purpose of navigation and orientation. The primary detection mechanism of this compass sense is uncertain but appears to originate from a truly quantum process involving spin-correlated radical pairs. In order to elicit sensitivity to weak magnetic fields, such as the Earth's magnetic field, the underlying spin dynamics must be protected from fast decoherence. In this work, we elucidate the effects of spin relaxation on a recently suggested reaction scheme involving three radicals, instead of a radical pair, doublet-quartet interconversion under magnetic interactions, and a spin-selective scavenging reaction. We show that, besides giving rise to a vastly enhanced reaction anisotropy, this extended reaction scheme is more resilient to spin relaxation than the conventional radical pair mechanism. Surprisingly, the anisotropic magnetic field effect can be enhanced by fast spin relaxation in one of the radicals of the primary pair. We discuss this finding in the context of magnetoreception. Radical scavenging can protect the spin system against fast spin relaxation in one of the radicals, thereby providing a credible model to the involvement of fast relaxing radical pairs, such as FADH^{\bullet} / $\text{O}_2^{\bullet-}$, in radical-pair based magnetoreception. This finding will help explain behavioural observations that seem incompatible with the previously proposed flavin semiquinone / tryptophanyl radical pair.

Introduction

A variety of animals, most notably many (migratory) birds, appear to employ a truly quantum mechanism to detect the geomagnetic field. In particular, evidence has accumulated that a light-dependent inclination compass is realized via spin-correlated radical pairs embedded in the animal's visual system – a hypothesis originally expressed by Schulten et al. as early as 1978 and later refined by Ritz, Adem and Schulten.¹⁻² While the sensory protein and the associated signalling cascade have not yet been identified unequivocally, the underlying radical pair (RP) is thought to derive from the blue-light photoreceptor cryptochrome.²⁻³ Several review articles summarize the astonishing animal behavioural, physiological and neurobiological studies that underlie our current understanding.⁴⁻¹⁰ The reader is referred to these works for a detailed account on the topic.

Magneto-sensitivity can result from a process that, according to the classical radical pair mechanism (RPM), entails three essential steps, which are summarized in

Figure 1a:¹¹⁻¹³ First, a RP is generated, typically in a pure spin state, e.g. $^1[A^{\bullet-} - B^{\bullet+}]$. *In vitro*, this step is realized by photoinduced electron transfer along three or four highly conserved tryptophan residues, the so-called tryptophan triad or tetrad, to the noncovalently bound, oxidized FAD cofactor.¹⁴⁻¹⁶ *In vivo*, the formation of the RP could result from the dark reoxidation of the fully reduced FAD, $FADH^-$, accumulated via an upstream light-dependent reduction route (e.g. see Figure 1 of ref ¹⁷ and Figure 5 of this work).¹⁷⁻²³ Second, the RP undergoes coherent singlet-triplet interconversion at a rate dictated by anisotropic hyperfine interactions with surrounding magnetic nuclei, the Zeeman interaction with the Earth's magnetic field, and the exchange and electron-electron dipolar coupling. Third, spin-selective reactions of the RP render the yield of a signalling state, which derives from the spin-correlated RP, dependent on the above-mentioned singlet-triplet interconversion process.

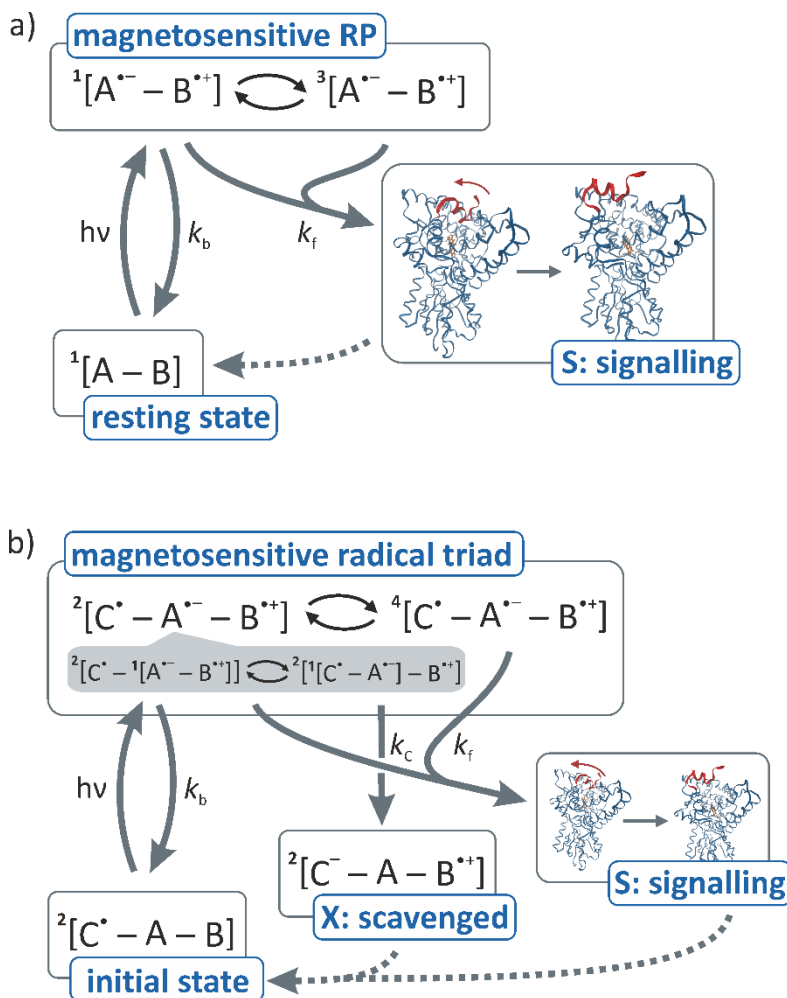


Figure 1: Generic reaction schemes of radical pair-based magnetoreception. a) Essential steps of the conventional RPM as applied to magnetoreception. b)

Scheme of magnetoreception extended to comprise a radical scavenging reaction of the primary RP. This scheme, introduced in ref²⁴, can give rise to vastly enhanced compass performance. Several different RPs have been discussed. $A^{\bullet-}$ is generally thought to derive from a cryptochrome-bound FAD, implying the semiquinoid radical $FAD^{\bullet-}$ or its protonated form, $FADH^{\bullet}$. $B^{\bullet+}$ appears to be more elusive; different schemes and radicals are discussed in the literature. C^{\bullet} is the scavenger radical.

Many theoretical studies have scrutinized the fundamental quantum physics of the RPM and established estimates of the expected size of the effect and its various limitations.^{11, 25-33} So far, these studies suggest that the quantum effect is in principle fit for purpose, albeit challenged by decoherence in noisy biological environments. However, inherently small directional responses may result as a consequence of inter-radical interactions and many not symmetry related hyperfine interactions.²⁷⁻²⁹ Recent comprehensive calculations for the $FAD^{\bullet-}/W^{\bullet+}$ RP reveal that the key quantity, the differences in the yield of signalling state at different field directions, might be perplexingly small.²⁷ The $FAD^{\bullet-}/Z^{\bullet}$ model (Z^{\bullet} is a hypothetical radical without hyperfine interactions) can provide larger anisotropies.^{27, 29} However, its only physical incarnation, the flavin/superoxide RP, has been refuted due to fast spin relaxation.³⁴ It is puzzling that in many respects the compass performance in animals surpasses these predictions (e.g. with respect to the acuity of the sensor, its function under very low light intensities, or its sensitivity to weak radio frequency magnetic fields), suggesting the presence of a powerful, yet unknown, amplification process and remarkable resilience to decoherence.^{4, 35}

We have recently proposed an extended reaction scheme, shown in Figure 1b, that is predicted to greatly (by a factor of 10 and more) enhance the compass sensitivity via the so-called “chemical Zeno effect”.^{24, 36} This model relies on a spin-selective reaction of one of the two radicals of the primary pair and a spin-bearing, external scavenger. This scavenger is initially uncorrelated with respect to the RP, a situation that resembles f-pairs, but eventually acquires correlation as a result of its spin-selective reactivity, i.e. the chemical Zeno effect.²⁴ It has been shown that this additional reaction induces singlet-triplet conversion in the original RP and serves as a spin-selective reaction channel.²⁴ As a consequence and contrary to previous theories, spin-selective recombination of the primary RP (step 3 in the above discussion) is no longer essential and the radicals could thus be farther apart than is necessary for efficient charge recombination. This means that tryptophan tetrads (rather than triads) or systems involving freely diffusing radicals can also give rise to sizeable magnetic field effects and that the detrimental effects of inter-radical exchange and dipolar interactions can be minimized.³⁷⁻³⁹ This aspect has been discussed in detail in our preceding publication.²⁴ The spin dynamics in these three-radical systems are characterized by doublet-quartet conversions (instead of the conventional singlet-triplet interconversions characteristic of the RPM). The doublet state can be formulated as singlet in the A/B- or A/C-manifold (labels

referring to radicals) in combination with a doublet radical, as shown in Figure 1b. These singlet substates are, however, *not* mutually exclusive, i.e. orthogonal. Three-spin systems have also been described in the context of spin catalysis and related studies of magnetic field effects (MFEs).⁴⁰⁻⁴³ These works are distinguished from the phenomena considered here by relying on the exchange coupling with otherwise unreactive spin catalysts. Here, the spin-selective reactivity of the radical scavenger is the characteristic interaction motif. This effect is also different from those discussed in refs⁴⁴⁻⁴⁵ (and partly labelled by the quantum Zeno effect), which rely on fast asymmetric recombination within the RP to enhance the compass performance (also see the discussion in ref²⁸).

In ref²⁴, we have anticipated that the amplifying effect of the radical scavenging reaction relies on slow spin relaxation in the scavenger (just as the conventional effect depends on slow relaxation in the radicals of the primary pair). If this criterion is not fulfilled, the scavenger is, just as a diamagnetic quencher, expected to merely reduce the RP lifetime and, hence, degrade the compass sensitivity rather than improve it. On the other hand, a few reports suggest that the RP-based compass can be enhanced or even entirely induced by spin relaxation.^{28, 46-47} As spin relaxation is an omnipresent consequence of environmental noise (e.g. dipole interactions, electron-electron distance fluctuations and reorientations and structural changes of the radicals brought about by thermal motion), it must not be disregarded in biological application of quantum mechanics.²⁷⁻²⁸ Here, we are set to elucidate the dependence of the amplification process on spin relaxation in the radicals.

Theory and Computational Details

We model the spin dynamics in systems comprising three radicals, henceforth referred to by the labels A, B and C. Radicals A^{•-} and B^{•+} are thought to form the primary RP, which in the conventional mechanism is the sole source of magnetosensitivity. C[•] takes the role of the scavenger, which, without loss of generality, reacts with A^{•-} in a spin-selective reaction producing the diamagnetic product **X**. The signalling state **S** is formed through a spin-independent pathway, e.g. proton transfer reactions and/or protein reorganisation, which is mutually exclusive to that yielding **X**. The dynamics of the system are assessed from the population weighted spin density operator in the combined Hilbert space of the three radicals, $\hat{\rho}(t, \Omega)$. It obeys the following equation of motion

$$\frac{d}{dt} \hat{\rho}(t, \Omega) = -i \left[\hat{H}(\Omega), \hat{\rho}(t, \Omega) \right] + \hat{K} \hat{\rho}(t, \Omega) + \hat{R} \hat{\rho}(t, \Omega), \quad (1)$$

which accounts for the coherent evolution under the Hamiltonian $\hat{H}(\Omega)$, reactions via the superoperator \hat{K} and spin relaxation via the superoperator \hat{R} . Neglecting inter-radical interactions (electron-electron exchange and dipolar couplings) for simplicity (see³⁹ for a motivation of and²⁸ for effects beyond this approach), $\hat{H}(\Omega)$ is the sum of the individual spin Hamiltonians, $\hat{H}_k(\Omega)$, of the three radicals. Here, $\hat{H}_k(\Omega)$ comprises the Zeeman interactions with the Earth-strength magnetic field

(of assumed 50 μT intensity; Larmor frequency: $g\mu_B/h\|\mathbf{B}_0(\Omega)\| = 1.4$ MHz) and hyperfine interactions with surrounding nuclear spins (in angular frequency units):

$$\hat{H}_K(\Omega) = g\mu_B\hbar^{-1}\mathbf{B}_0(\Omega)\cdot\hat{\mathbf{S}}_K + \sum_j^{N_K}\hat{\mathbf{S}}_K\cdot\mathbf{A}_{Kj}\cdot\hat{\mathbf{I}}_{Kj}. \quad (2)$$

$\hat{\mathbf{S}}_K$ and $\hat{\mathbf{I}}_{Kj}$ are the angular momentum operators of electron spin $K \in \{A, B, C\}$ and of nuclear spin j in radical K , respectively. The sum runs over all N_K magnetic nuclei with hyperfine tensor \mathbf{A}_{Kj} in radical K . Ω denotes the polar and azimuthal angles of the external magnetic field, $\mathbf{B}_0(\Omega)$, in the coordinate frame of the protein. The geomagnetic field is weak enough that, for organic radicals, the differences in g -factors of the three electron spins can safely be neglected (in particular, $g \approx 2$).

The superoperator \hat{K} accounts for all reactions of the radical triad. Specifically, following the Haberkorn approach,⁴⁸ \hat{K} is given by

$$\hat{K}\hat{\rho}(t, \Omega) = -\frac{1}{2}k_c[\hat{P}_{AC}^S, \hat{\rho}(t, \Omega)]_+ - \frac{1}{2}k_b[\hat{P}_{AB}^S, \hat{\rho}(t, \Omega)]_+ - k_f\hat{\rho}(t, \Omega) \quad (3)$$

and describes the spin-selective scavenging reaction that forms \mathbf{X} (rate constant k_c) from the reaction of A^{*-} and C^* , the charge recombination of A^{*-} and B^{*+} (rate constant k_b), and the generation of the signalling state \mathbf{S} in a spin-independent reaction (rate constant k_f).⁴⁸ \hat{P}_{KL}^S is the singlet projection operator in the subspace of the electron spins of K and L :

$$\hat{P}_{KL}^S = \frac{1}{4}\hat{I} - \hat{\mathbf{S}}_K \cdot \hat{\mathbf{S}}_L. \quad (4)$$

Note that here we focus on radical scavenging reactions and assume a diamagnetic product state \mathbf{X} , i.e. no triplet quenching product is formed. For organic molecules, the latter is normally an excited state, which is populated at a lower rate. More general scenarios have been discussed in²⁴.

Spin relaxation is modelled by the trace-preserving and completely positive Lindblad form

$$\hat{R}\hat{\rho}(t, \Omega) = \sum_n \gamma_n \frac{1}{2} \left(2\hat{A}_n\hat{\rho}(t, \Omega)\hat{A}_n^\dagger - \hat{\rho}(t, \Omega)\hat{A}_n^\dagger\hat{A}_n - \hat{A}_n^\dagger\hat{A}_n\hat{\rho}(t, \Omega) \right), \quad (5)$$

with the sum running over the set of operators $\hat{A}_n \in \{\hat{S}_{K,x}, \hat{S}_{K,y}, \hat{S}_{K,z}\}$ for every relaxing electron spin K . This gives a total of nine different noise operators. Assuming, as we do here, that the coupling coefficients γ_n are the same for the three (uncorrelated, i.e. incoherently modulated) spatial dimensions, i.e. for $\hat{A}_n = \hat{S}_{K,x}$, $\hat{S}_{K,y}$ and $\hat{S}_{K,z}$ individually, this approach gives rise to the random-field relaxation superoperator, popular in electron or nuclear spin resonance, with equal spin-lattice (T_1) and spin-spin relaxation times (T_2), i.e. $\gamma_K = T_{1,K}^{-1} = T_{2,K}^{-1}$. In this scenario, eq. (5) can also be rewritten as:

$$\hat{R}\hat{\rho}(t,\Omega) = \sum_K \gamma_K \left(\sum_{i \in \{x,y,z\}} S_{K,i} \hat{\rho}(t,\Omega) S_{K,i} - \frac{3}{4} \hat{\rho}(t,\Omega) \right). \quad (6)$$

Nuclear relaxation can be neglected because it occurs on a much slower time scale. Eq. (5) is a physically reasonable generic model in which both phase and amplitude are perturbed, with equal probability, by a stochastic memoryless, i.e. Markovian, process.^{30, 46, 49-50} The relaxation rates can be related to the variance of the amplitude of the noise fields.²⁸ The Lindblad form preserves the physicality of the density operator even for exceedingly fast spin relaxation. Based on results from³⁰, we do not anticipate a qualitative difference between this model and models that also include noise on the nuclear spins or correlated noise. Alternatively, less generic descriptions based on the Redfield approach have recently been used.²⁷⁻²⁸ However, given the yet unknown identity and motional properties of C*, this can only be a topic for future studies.

Eq. (1) is solved for the initial condition

$$\hat{\rho}(0,\Omega) = \hat{P}_{AB}^S / \text{Tr}[\hat{P}_{AB}^S], \quad (7)$$

which corresponds to a singlet configuration in the A⁻/B⁺-pair and a uncorrelated C*. This is the configuration expected to prevail in RPs generated by swift electron transfer reactions from diamagnetic A/B-precursors in the presence of an unpolarised C*. We also consider a reaction initiated by electron transfer from the fully reduced FADH⁻ to triplet oxygen, in which case the singlet projector operator \hat{P}_{AB}^S in eq. (7) is to be swapped by the triplet projection operator, $\hat{P}_{AB}^T = \hat{I} - \hat{P}_{AB}^S$.

The quantum yield of the signalling state **S**, once all radicals have reacted, is given by

$$\gamma_s(\Omega) = k_f \int_0^\infty \text{Tr}[\hat{\rho}(t,\Omega)] dt = k_f \text{Tr}[\hat{\rho}(\Omega)], \quad (8)$$

with $\hat{\rho}(\Omega) = \int_0^\infty \hat{\rho}(t,\Omega) dt$ denoting the accumulated density operator. The directional dependence of the yield dictates the performance of the reaction as a compass sensor. Here, we define two measures: the absolute (Δ_s) and the relative (Γ_s) anisotropy of the yield of the signalling state **S**:

$$\Delta_s = \max_{\Omega} [\gamma_s(\Omega)] - \min_{\Omega} [\gamma_s(\Omega)], \quad (9a)$$

$$\Gamma_s = \frac{\Delta_s}{\langle \gamma_s \rangle} \quad \text{where} \quad \langle \gamma_s \rangle = \frac{1}{4\pi} \int \gamma_s(\Omega) d\Omega. \quad (9b)$$

It is not currently clear which of Δ_s and Γ_s corresponds more closely to what animals perceive when they take a magnetic compass bearing. It has been argued that Γ_s might be more relevant, because as an intensive quantity it is insensitive to the total number of excited/chemically produced RPs.⁴ On the other hand it seems obvious that a certain absolute concentration change Δ_s will be required to feed into down-stream amplification cascades without being marginalized by thermal

fluctuations. The corresponding quantities, Δ_X and Γ_X , for the yield of the scavenging product **X** can be evaluated in a similar fashion.

Results

In the following, we explore the effects of spin relaxation on the ability of radical scavenging reactions to amplify the absolute and the relative anisotropy of the yield of the signalling state, Δ_S and Γ_S . We focus on two simple prototype RP models of the $FAD^{\bullet-}/Z^{\bullet-}$ and the $FAD^{\bullet-}/W^{\bullet+}$ -type. For $FAD^{\bullet-}$, we retain the two ^{14}N hyperfine interactions modelled after the N5 and N10 nitrogens; for $W^{\bullet+}$, the ^{14}N hyperfine interaction associated with the N1 nitrogen is modelled (hyperfine tensors given in the Supporting Information). $Z^{\bullet-}$ is a radical without hyperfine interaction. Our choice of model is motivated by reasonable simplicity and the desire to provide continuity with previous theoretical papers. Hyperfine tensors and the relative orientation of the radicals were taken from ref ²⁴, where these models were used to introduce the phenomenon of scavenging-enhanced magnetic field effects. This work also revealed that the amplification effect is remarkably invariant to enlarging the spin system in any of the radicals, thereby suggesting that the studied models, though simple, are nonetheless representative. The forward rate constant k_f was fixed at $0.1 \mu s^{-1}$, yielding a RP lifetime of $10 \mu s$ in the absence of spin-selective charge recombination or scavenging. This is motivated by a recent study of spin relaxation in AtCry, suggesting that the MFEs would be strongly attenuated for longer-lived RPs.²⁷ The charge recombination rate constant, k_b , was varied in the range 0 to 2 and its value is reported as $\varphi = k_b/k_f$. In an *in vitro* study, φ was found to be ~ 2 for AtCry.¹⁴ The external magnetic field had an intensity of $50 \mu T$ and inter-radical interactions were neglected. The scavenger was assumed to react with the $FAD^{\bullet-}$ radical. In the Discussion, we will apply the conclusions of our study to magnetoreception, for which the identity of the magneto-sensitive RP is currently unknown. In fact, no RP-model is presently known that is both, in agreement with all experimental findings and not hampered by fast spin relaxation.^{4, 17, 34} Yet, we anticipate that our findings readily generalize to these potentially complex systems. In particular, we have shown in ref ²⁴ that *in the presence of radical scavenging* the magnetic field anisotropy is only weakly influence by the hyperfine coupling constants in $B^{\bullet+}$. Consequently, comparable results are expected for the $FAD^{\bullet-}/Z^{\bullet-}$ and the $FAD^{\bullet-}/W^{\bullet+}$ model under conditions of radical scavenging. Note in this context that recent evidence is refuting the involvement of a $FAD^{\bullet-}/W^{\bullet+}$ -based radical in magnetoreception in birds.¹⁷ Nevertheless, $FAD^{\bullet-}/W^{\bullet+}$ is relevant in terms of providing a model that is potentially testable in *in vitro* experiments.¹⁴

Effects of concomitant electron spin relaxation in all radicals

We commence by discussing the dependence of the reaction-amplified anisotropy on the decoherence rate for the model of random-field relaxation (see eq. (6)) involving all three electron spins with identical (but uncorrelated) rates: $\gamma = \gamma_A = \gamma_B = \gamma_C$. Figure 2a/b shows Γ_S as a function of k_C in the absence (solid lines) and presence (dashed lines) of relaxation. The corresponding data for Δ_S are plotted in

Figure S1 in the Supporting Information. These curves reflect the general characteristics of the effect, which for the no-relaxation scenario have already been discussed in ref²⁴. In brief, the compass performance is markedly enhanced by the radical scavenging reaction, the maximum for Γ_s occurring at larger k_c ($\sim 50 \mu\text{s}^{-1}$ for $\varphi = 0$) than that for Δ_s (at $\sim 5 \mu\text{s}^{-1}$ for $\varphi = 0$). Note that for $\varphi = 0$, i.e. in the absence of an efficient spin-selective charge recombination reaction, the MFE vanishes in the absence of the radical scavenging reaction ($k_c \rightarrow 0$), while both Δ_s and Γ_s can be substantial in its presence. These qualitative features apply in idealized, i.e. static and relaxation-free ($\gamma = 0$), as well as in noisy environments ($\gamma > 0$; dashed lines). Note furthermore that the identity of $B^{*\cdot}$, i.e. Z^* (Figure 2a) or $W^{*\cdot}$ (Figure 2b), does not have a bearing on the functioning of the scavenging mechanism. In fact, the reaction anisotropies nearly coincide for $k_c > 1 \mu\text{s}^{-1}$, both with and without relaxation (see Figure S2 in the Supporting Information for an overlay of the Γ_s -values for $FAD^{*\cdot}/Z^*$ and $FAD^{*\cdot}/W^{*\cdot}$). For the relaxation-free systems, this agreement was anticipated based on results from ref²⁴. In Figure 2, the effect of spin relaxation at a rate fast compared to the RP lifetime is shown, i.e. $\gamma = 1 \mu\text{s}^{-1}$. Under this condition, the maximal Γ_s is reduced by an approximate factor of 5 while the maximal Δ_s is diminished by a full order of magnitude. It is furthermore noteworthy that for significant radical quenching in the presence of relaxation, the variability with φ is significantly reduced, while in the absence of relaxation small $\varphi \rightarrow 0$ give rise to larger Δ_s and Γ_s . The scavenging rates for the maximal effect shift to slightly smaller and larger k_c for Γ_s and Δ_s , respectively. Figure 2c/d illustrates the dependence of the performance parameters on the relaxation rate γ for $k_c = 0 \text{ s}^{-1}$ (no scavenging, dashed-dotted lines) and $k_c = 51.8 \mu\text{s}^{-1}$ (solid lines). The latter rate approximately corresponds to the maximum in Γ_s for $\varphi = 0$ in the absence of relaxation. These graphs once again reveal the weak dependence on φ in the presence of fast relaxation. It is obvious that the scavenging effect enhances the resilience of the MFE to relaxation: If we assume, as a matter of illustration, that $\Gamma_s = 0.01$ is sufficient for the compass to function, the scavenged $FAD^{*\cdot}/W^{*\cdot}$ RP would be able to tolerate an approximately 40 times faster relaxation rate than the isolated RP for $\varphi = 2$ (i.e. $\gamma = 20 \mu\text{s}^{-1}$ for the scavenged RP at any φ vs. $0.5 \mu\text{s}^{-1}$ for the isolated RP with $\varphi = 2$). For $FAD^{*\cdot}/Z^*$, an approximately 14 times larger relaxation rate is tolerable. In this comparison, we have chosen the favourable value of $\varphi = 2$, which has been found for AtCry *in vitro*.¹⁴ In animal cryptochromes, the tryptophan triad would give rise to smaller value of φ on account of a larger inter-radical distance (however, a mechanism different from electron transfer along the triad/tetrad could be relevant *in vivo*).^{15, 37-38} Qualitatively similar comments apply to Δ_s (Figure S1); the enhancing effect is however smaller: if we stipulate that an absolute change of 1 % of the excited population is necessary to elicit a reliable compass bearing, we find that radical scavenging allows the compass to tolerate a 6 times larger γ for $FAD^{*\cdot}/W^{*\cdot}$ (2 times larger for $FAD^{*\cdot}/Z^*$).

It is interesting to note that the improved resilience to relaxation does not only originate from the sheer magnitude of the effect in the presence of scavenging, but in part results from an inherently weaker susceptibility to noise. This conclusion is

supported by plotting $\Gamma_s(k_c=51.8 \mu\text{s}^{-1})/\Gamma_s(k_c=0)$ vs. γ (see Figure S3 in the Supporting Information). A constant value would be expected if the relaxation behaviours was of the same functional form for both values of k_c . However, the plot reveals a constant ratio for small γ followed by a marked maximum at intermediate γ , indicative of a relative slow-down of the degradation of Γ_s -performance in the presence of radical scavenging.

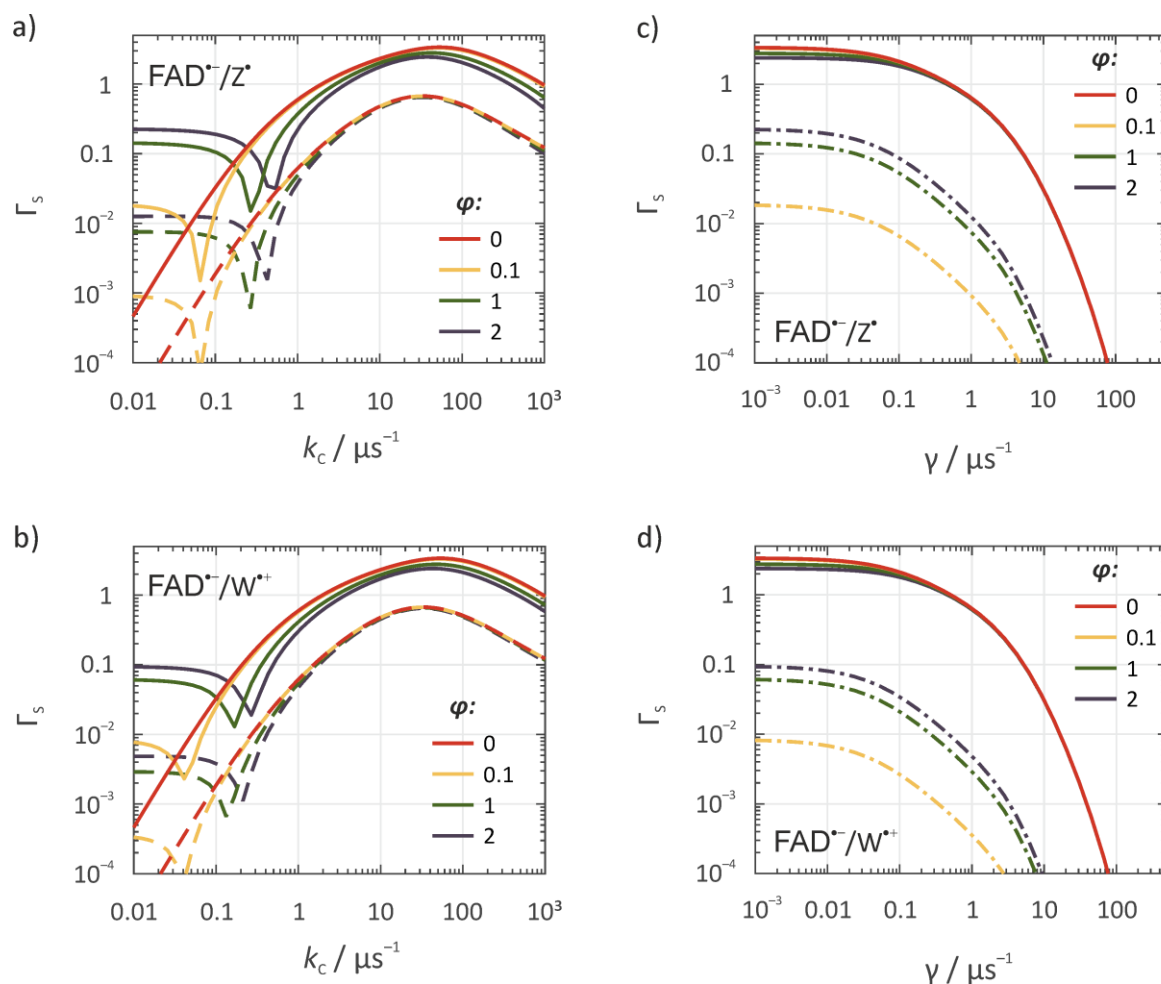


Figure 2: Compass performance as a function of k_c or γ . *a) and b)*: Dependence of Γ_s on k_c in the absence (solid lines) and presence (dashed lines) of spin relaxation with $\gamma = \gamma_A = \gamma_B = \gamma_C = 1 \mu\text{s}^{-1}$ for various $\varphi = k_b/k_f$ as encoded by the different colours and summarized in the common legends. *c) and d)* Dependence of Γ_s on $\gamma = \gamma_A = \gamma_B = \gamma_C$ for $k_c = 51.8 \mu\text{s}^{-1}$ (solid lines) and $k_c = 0 \text{ s}^{-1}$ (no scavenging, dashed-dotted lines). For $\varphi = 0$, the MFE vanishes for the conventional RP model in the absence of spin-selective recombination. All calculations are based on a spin system comprising N5 and N10 of $\text{FAD}^{\bullet-}$ in $\text{A}^{\bullet-}$ and no hyperfine coupled nuclei in C^{\bullet} . For panels *a) and c)* no hyperfine coupled nuclei are present in $\text{B}^{\bullet+}$ ($\text{FAD}^{\bullet-}/\text{Z}^{\bullet+}$ model); for panels *b) and d)* N1 of $\text{W}^{\bullet+}$ has been included ($\text{FAD}^{\bullet-}/\text{W}^{\bullet+}$ model). $B_0 = 50 \mu\text{T}$ and $k_f = 0.1 \mu\text{s}^{-1}$. Figure S1 in the Supporting Information provides the corresponding plots for Δ_s .

Effects of electron spin relaxation in individual radicals

As it is unlikely that all electron spins relax at the same rate, we continued our exploration by investigating the sensitivity of the compass performance to relaxation in *individual* radicals. Figure 3 summarizes our results for various φ and $k_c = 51.8 \mu\text{s}^{-1}$, i.e. the scavenging rate corresponding to the maximum in Γ_s for $\varphi = 0$ in the absence of relaxation.

In the scenarios that either radical $A^{\bullet-}$ or radical C^{\bullet} relax while the two other radicals are unperturbed by the noisy environment, the dependence of Δ_s and Γ_s on γ qualitatively follows the trend outlined above for simultaneously relaxing $A^{\bullet-}$, $B^{\bullet+}$ and C^{\bullet} (see Figure 3 and S4 and S5 in the Supporting Information). Expectedly, the effect of γ is weaker if only one of the radicals is relaxing as opposed to all radicals: in the A-only or C-only scenario, roughly twice the γ is generating the same relaxation degradation as observed for all-radical relaxation. Furthermore, it is virtually irrelevant whether radical $A^{\bullet-}$ or C^{\bullet} is relaxing; the corresponding curves for Γ_s and Δ_s in Figures 3 and S4 are basically superimposed (except for very fast relaxation, $\gamma > 100 \mu\text{s}^{-1}$, for which, however, the anisotropy is impracticably small; not shown). The surprising aspect of these data is the fact that fast relaxation in $B^{\bullet+}$ does not degrade the compass performance (see green lines in Figure 3). In fact, for $\varphi > 0$ it enhances, instead of diminishes, both Δ_s and Γ_s , while, for $\varphi = 0$, relaxation in $B^{\bullet+}$ does not have a significant effect at all. As a consequence, if $B^{\bullet+}$ and C^{\bullet} relax simultaneously (at the same rate $\gamma_B = \gamma_C = \gamma$; dashed-dotted line in Figure 3), the performance curve follows that for relaxing C^{\bullet} (C^{\bullet} -only) for $\varphi = 0$, while a small enhancement over that of C-only results for $\varphi > 0$. This is another example of relaxation-enhanced compass performance.^{28,46} Along similar lines, spin relaxation in $A^{\bullet-}$, $B^{\bullet+}$, and C^{\bullet} gives rise to a slightly better sensitivity than is observed for relaxation in $A^{\bullet-}$ and C^{\bullet} alone (see Figure S5 in the supporting Information). It is noteworthy that even though $B^{\bullet+}$ might relax swiftly, its presence is crucial to the overall enhancement; in the isolated $A^{\bullet-}/C^{\bullet}$ -system, Γ_s is only of the order of 0.1 even under favourable conditions with respect to φ and lifetime. Note furthermore that the enhancing effect is not *per se* attributed to the annihilation of the hyperfine interactions in $B^{\bullet+}$ by fast spin relaxation.^{29, 51} In particular, a similar enhancing effect as for the $FAD^{\bullet-}/W^{\bullet+}$ scenario is found for a three-radical system with no hyperfine coupling interactions within $B^{\bullet+}$ ($FAD^{\bullet-}/Z^{\bullet}$ model; see Figure 3b and Figure S4 in the Supporting Information; the agreement is particularly striking for Γ_s at $k_c = 51.8 \mu\text{s}^{-1}$). Having said that, the asymptotic value of Δ_s or Γ_s reached for fast relaxation in $B^{\bullet+}$ is indeed independent of the hyperfine coupling interactions in $B^{\bullet+}$, i.e. the picture of annihilated hyperfine interaction does nonetheless have some validity.

In general, the origin of the effect is difficult to elucidate as the simplest model already comprises a total of four spins. A conceptual understanding can be gained by reference to a simple model for which $A^{\bullet-}$ comprises a single nuclear spin-1/2 with hyperfine tensor characterized by the principal values $A_{xx} = 0$, $A_{yy} = 0$ and $A_{zz} \neq$

0 (and typically large) and no hyperfine interactions in B^{*+} and C^* . Note that the hyperfine pattern is indeed realized in good approximation for the N5 and N10 nitrogen atoms in the flavin radical. For $\varphi = 0$, this model can be analysed in sufficient detail to reveal the inner working of the scavenging process, as has been shown in ref ²⁴. For completeness, we reiterate the argument: For general orientations of the magnetic field, one finds that the Liouvillian comprises two relevant blocks (parametrized by the nuclear spin quantum number of the nucleus in A^{*-}). All singlet and triplet configurations of the A/B-pair are coherently or incoherently (i.e. through kinetics) coupled. As a consequence, for a fast scavenging reaction (faster than k_b), nearly the entire radical triad population is eventually deactivated by scavenging and the yield of the signalling state is correspondingly low. This applies for all magnetic field orientations except for its alignment with the molecular z-axis. In this case, the Hamiltonian factors (it now only connects T_0 and S in the A/B-manifold) and so does the Liouvillian (which is characterized by blocks comprising e.g. the $S\alpha$, $T_0\alpha$ and $T_+\beta$ -populations, the labels referring to the combined spin state in the A/B-manifold and the scavenger spin). In this situation, the scavenging reaction populates states that are inaccessible to further scavenging (as discussed in ref ²⁴; cf. Figure 3 in this reference) and thus fated to generate the signalling state in a spin-independent transformation. As a consequence, the yield of the signalling state is large for this and only for this orientation. In the absence of relaxation, this unreactive subspace (i.e. the null space of the Liouvillian) comprises the S and T_0 -populations of the A^{*-}/B^{*+} -pair (in addition to the coherences involving these states and for any spin state of the scavenger radical), while in the presence of relaxation in B^{*+} , this subspace is enlarged to also comprise the $T_+\alpha$ and $T_-\beta$ -populations. The spin-selective A^{*-}/B^{*+} -recombination can partly, i.e. via the S-state, deplete this subspace, thereby competing with the generation of the signalling state. On account of the coherent coupling of T_0 and S, this depletion is more efficient in the absence of B^{*+} -relaxation than in its presence, because in the latter case the population is spread over a larger number of A^{*-}/B^{*+} -unreactive states, i.e. the $T_+\alpha$ and $T_-\beta$ -populations, of the enlarged subspace. As a consequence, the yield of the signalling state is larger in the presence of relaxation and so is Γ_S .

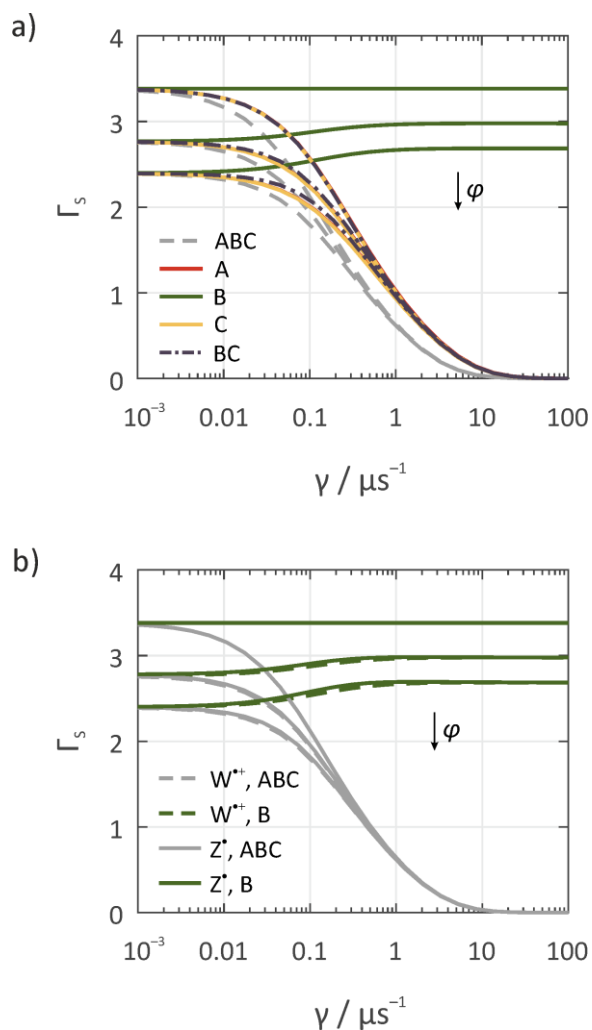


Figure 3: Dependence of Γ_s on the rate of random-field spin relaxation in chosen parts of the three-radical system for $\phi = k_b/k_f = 0, 1,$ and 2 . Panel *a)* applies to the scavenged $\text{FAD}^{\bullet-}/\text{W}^{\bullet+}$ scenario. The relaxing radicals are colour-coded. The red lines (spin relaxation in $\text{A}^{\bullet-}$) are effectively superimposed by the yellow lines corresponding to spin relaxation in C^{\bullet} . In panel *b)* the $\text{FAD}^{\bullet-}/\text{W}^{\bullet+}$ model is compared to the $\text{FAD}^{\bullet-}/\text{Z}^{\bullet}$ model: For the dashed lines, radical $\text{B}^{\bullet+}$ comprised a single hyperfine interaction (modelled after N1 of $\text{W}_C^{\bullet+}$); for the solid lines, $\text{B}^{\bullet+}$ is of the Z^{\bullet} -type with no coupled magnetic nuclei. These two families of curves effectively coincide. Random-field spin relaxation is present in $\text{B}^{\bullet+}$ (green lines) or in all radicals of the three-radical systems (grey lines). All simulation parameters are the same as for Figure 2; $k_C = 51.8 \mu\text{s}^{-1}$.

A more systematic study of the dependence of Γ_s on the relaxation rates for various k_C reveals the broad applicability of radical scavenging to enhance the compass performance. Figure 4 summarizes our results for Γ_s . In this figure, our arbitrary decisive criterion $\Gamma_s = 1\%$ has been indicated by white contour lines. In

brief, a remarkable enhancement of Γ_s is observed for k_c ranging from $1 \mu\text{s}^{-1}$ to $1000 \mu\text{s}^{-1}$. In this region, spin relaxation rates of up to $10 \mu\text{s}^{-1}$ (refer to Figure 4 for details) can be accommodated for $A^{\bullet-}$ or C^{\bullet} while sustaining a compass sensitivity that often surpasses that of the conventional RP model in the absence of relaxation. It is interesting to note that for $\varphi > 0$, the k_c -region of enhanced compass performance, i.e. $1 \mu\text{s}^{-1} < k_c < 1000 \mu\text{s}^{-1}$, is separated from the low- k_c limit, i.e. $k_c < 0.01 \mu\text{s}^{-1}$, by a dip in Γ_s . In this region of intermediate radical scavenging ($k_c \sim 0.1 \mu\text{s}^{-1}$), the compass performance is reduced compared to the conventional model. This is an important realization, as it stresses the necessity of an efficient scavenging reaction pathway connecting $A^{\bullet-}$ and C^{\bullet} . For moderate to fast radical scavenging, spin relaxation in $B^{\bullet+}$ is found to be inconsequential or even performance enhancing. Only for low scavenging rates, for which the model reduces to the conventional RP model, is spin relaxation in $B^{\bullet+}$ performance degrading. On the other hand, spin relaxation in C^{\bullet} is (expectedly) only relevant for fast to moderate scavenging. Qualitatively analogous comments apply to the dependence of Δ_s on k_c and γ (see Figure S6 in the Supporting Information). For the region of significant scavenging, $1 \mu\text{s}^{-1} < k_c < 1000 \mu\text{s}^{-1}$, the $FAD^{\bullet-}/Z^{\bullet}$ and the $FAD^{\bullet-}/W^{\bullet+}$ model yield comparable reaction anisotropies.

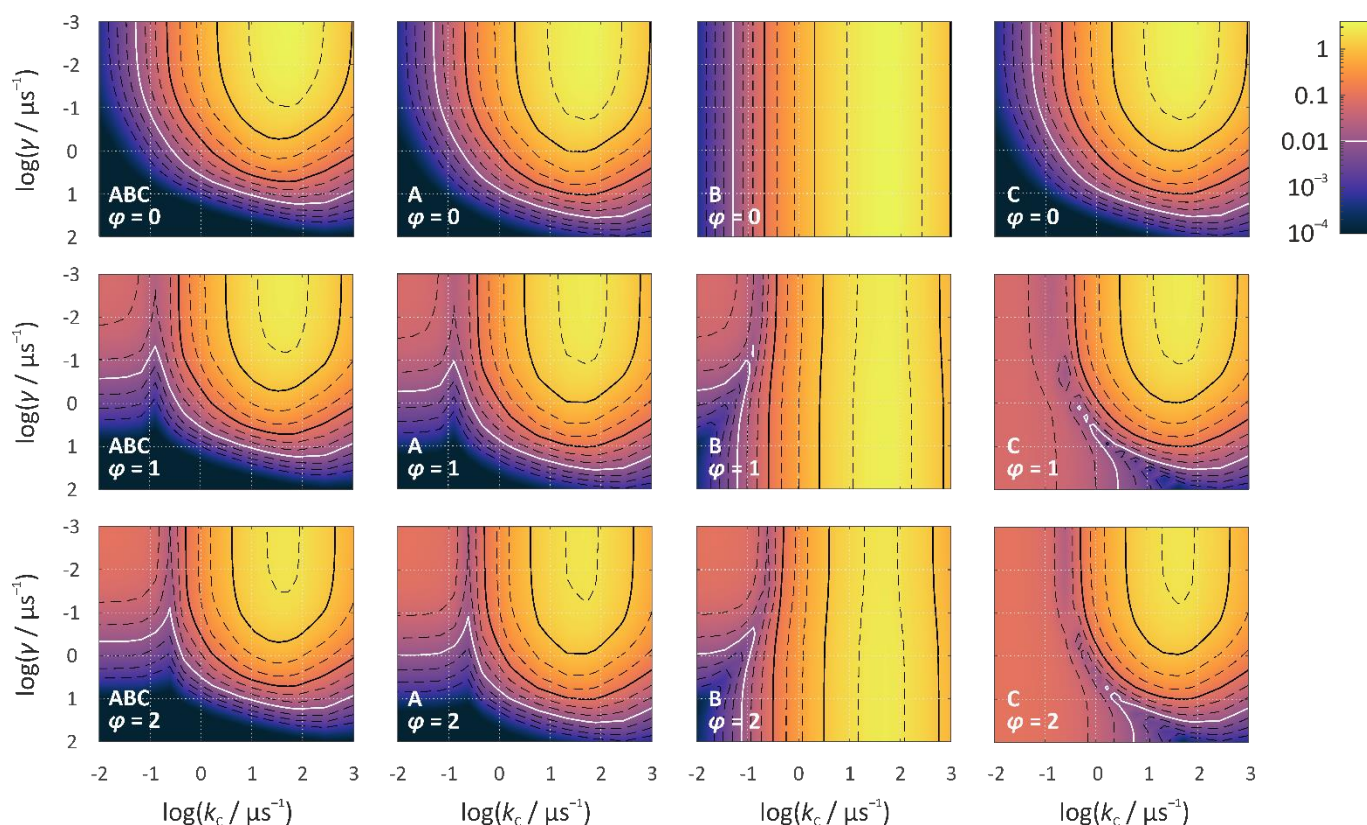


Figure 4: Contour plots of Γ_s as a function of k_c and γ for three different $\varphi = 0, 1$, and 2 (rows) and random field relaxation in all three radicals (left) or either $A^{\bullet-}$, $B^{\bullet+}$, or C^{\bullet} (right), here labelled A, B and C, respectively. The contour lines and colour

shades correspond to a logarithmic scale. The white and the two solid black contour lines corresponds to 1 %, 10 % and 100 %. The 1 % contour is used in the main text to discuss the resilience of the compass to spin relaxation. A⁻, B⁺ and C[•] comprised N5 and N10 of FAD⁻, N1 of Wc^{•+} and no magnetic nuclei, respectively. All simulation parameters were the same as for Figure 2.

Discussion

Spin-selective scavenging can dramatically boost the relative and absolute anisotropy in the absence as well as the presence of spin relaxation. The remarkable resilience to fast relaxation in the second radical, B⁺, which, for $k_b > 0$ even affords relaxation-enhancement, widens the scope of the RPM to include constituent radicals with spin relaxation rates that are too fast to elicit a significant MFE via the conventional RPM. In the context of magnetoreception, this prospect appears particularly relevant to reaction schemes involving the superoxide radical, which have been advocated by several studies but suffers from fast spin relaxation.^{17-23, 34} Below, we will give a short account on magnetoreception involving superoxide and discuss one of its main issues, fast spin relaxation. We will then demonstrate how a radical scavenging reaction can be used to principally overcome this inherent obstacle. Our discussion of a possible realization of this mechanism through radical scavenging is by necessity speculative, and alternatives cannot be excluded.

Magnetoreception involving superoxide

The photocycle underlying magnetoreception has not yet been unequivocally identified. MFE studies on isolated cryptochromes and closely related photolyases have ascribed the magnetosensitivity to the RP [FAD⁻/W^{•+}], produced through a sequence of swift electron transfer steps involving the tryptophan triad.^{14-15, 52} The transferability of this finding to *in vivo* conditions has been questioned by several behavioural and histochemical studies suggesting that the key step involves the reoxidation of the fully reduced FADH⁻, likely by molecular oxygen.¹⁷⁻²³ Support for this hypothesis is predominantly drawn from the light dependence of the compass sense: Birds, pre-exposed to white light, could orient under green light (approximately 560 nm) even though oxidized FAD is not excitable below approximately 500 nm.^{18, 21, 53-54} This finding has been attributed to the secondary photoreduction of the semiquinone radical FADH[•] to FADH⁻, which can indeed be facilitated by green light. Along the same lines, histochemical studies suggested that Cry1a in the retina of chickens could be photoactivated by green light and that structural changes connected to the C-terminal region of the cryptochrome, which could be relevant in signalling, are triggered in the fully reduced form.¹⁹⁻²⁰ It was also argued that the efficient charge separation in animal cryptochromes and closely related animal (6-4) photolyases containing a tryptophan tetrad would preclude magnetosensitivity in the photoinduced flavin-tryptophan RPs, because the rate of spin-selective recombination was too low.³⁷⁻³⁸ While this argument was

expressed in favour of dark-state RP generation, this issue could in principle be overcome by radical scavenging of the RP of the forward reaction as we described it in ref ²⁴. The strongest evidence is provided by a recent behavioural study employing interleaved light and magnetic field pulses.¹⁷ The astonishing observation that the tested birds were oriented despite no temporal overlap in light and magnetic field could imply that the magnetosensitive RP is formed in a light-independent reaction. The only currently hypothesised RP that may potentially explain these results is FADH[•]/O₂^{•-}, generated in the reoxidation of the fully (photo)reduced FADH⁻. It is also interesting to note that the substitution of the third tryptophan of the conserved tryptophan triad by phenylalanine does not abolish the MFE for *Drosophila melanogaster* in behavioural studies⁵⁵ and in single-channel recordings of the depolarization of the membrane potential in motoneurons ectopically expressing cryptochrome.⁵⁶ As alternative (but less efficient) pathways of photoreduction exist and are known to be active *in vivo*, the dark reoxidation is an interesting hypothesis to rationalize these findings in terms of a single, well defined RP.⁵⁷⁻⁵⁸

The FADH[•]/O₂^{•-}-model is principally endowed with a favourable property: the anisotropy of the singlet yield is markedly (by an order of magnitude) larger in RPs combining FAD with a partner radical with no significant hyperfine interactions, such as O₂^{•-}, or better a hypothetical variety of it not subject to fast spin relaxation, conventionally denoted Z[•].^{27, 29} The Z[•]-hypothesis could also rationalize the observation of remarkable sensitivity of birds to perturbing radio frequency magnetic fields at the Zeeman resonance (the Larmor precession frequency of a free electron spin in the geomagnetic field), provided (incomprehensibly) long coherence times could be realized in the birds and that inter-radical interactions are insignificant.^{22, 59-60} While recent studies by the Mouritsen group challenge the idea of the Zeeman-resonance by demonstrating that broadband noise could be more disruptive,⁶¹⁻⁶² these findings do not by themselves contradict the superoxide hypothesis ⁶³. In any case, FADH[•]/O₂^{•-} does have many virtues despite a longstanding history of debates and remaining questions.

However, there is one seemingly unsurmountable flaw to the simple FADH[•]/O₂^{•-} model: fast spin relaxation.^{34, 64} Due to its orbital structure, O₂^{•-} is characterized by huge *g*-tensor anisotropy, which induces spin relaxation in the rotationally tumbling molecule. At weak magnetic fields, the dominant relaxation mechanism is spin-rotational relaxation, for which γ is proportional to τ_c^{-1} , the inverse rotational correlation time, i.e. the relaxation rate decreases with decreasing rate of rotational diffusion. While a detailed account of relaxation in O₂^{•-} is beyond the scope of this work (see refs ³⁴ and ⁶⁴ for details), here it suffices to observe that this mechanism predicts $\gamma = 1.8 \cdot 10^9 \text{ s}^{-1}$ for aqueous solutions even in the scenario of strong solvent/matrix-interactions (i.e. assuming a ratio of spin-orbit coupling constant to ligand-field splitting of -0.1 as inferred from cryogenic measurements; see ⁶⁴). Indeed, no MFEs on reactions of superoxide have been documented at low magnetic fields (effects are, however, possible for fields of several Tesla for which the rate of spin-mixing by the Zeeman interaction is comparable to the spin relaxation rates).⁶⁴ Due to the fact that intracellular viscosity is expected to be markedly higher than that of water (dynamic viscosity of hydrophobic cellular

compartments: 80 mPa s vs. 1 mPa s for water),⁶⁵ correspondingly slower spin relaxation rate might apply under biologically relevant conditions. However, the estimated rate of $\gamma = 2.2 \cdot 10^7 \text{ s}^{-1}$ (i.e., $\gamma^{-1} = 45 \text{ ns}$) is still too fast as to provide the required sensitivity to the geomagnetic field. In fact, RP lifetimes of the order of microseconds (which have been found for AtCry *in vitro* but did not elicit a sensitive response to Earth-strength magnetic fields¹⁴) would require spin relaxation rates smaller by at least a factor of 22; to approach the lifetimes suggested by the radio frequency MFEs on birds,^{22, 59-62, 66} a factor of the order 10^4 is at odds.³⁰ In line with these observations, no MFE could be detected for the FADH[•]/HOO[•] RP in pyranose 2-oxidase from *Trametes multicolour* up to 160 mT.⁶⁷ Taken together, this demonstrates that isolated RPs involving O₂^{•-} are generally incompatible with a viable (directional) response to the Earth's magnetic field through the classical RP mechanism.

Magnetoreception involving superoxide and radical scavenging

The restrictions related to fast spin relaxation of superoxide do *not* necessarily apply to superoxide-containing RPs under the influence of radical scavengers. As shown above, fast spin relaxation is unproblematic or, in view of potential relaxation enhancement, even desired if the swiftly relaxing radical assumes the role of B^{•+}. The reaction scheme could thus entail the oxidation of the fully reduced FADH⁻ with O₂ to form FADH[•]/O₂^{•-} in the overall triplet state or, although this does not seem to be supported by experimental evidence, the random encounter of O₂^{•-} and a cryptochrome already containing the semiquinone FADH[•].⁶⁸ In any case, these reactions must occur in the presence of a scavenger radical C[•]. The fact that the A^{•-}/B^{•+}-RP is formed in the triplet state or as F-pair is mostly inconsequential to the predicted enhancement. As we show in the Supporting Information (cf. Figure S7 in the Supporting Information), huge anisotropies are found independent of the initial spin configuration in the AB-manifold. Likewise, for the scavenged system, the “polarity” of the reaction yield does not depend on the initial configuration, i.e. larger (compared to the average) yields of the signalling states are always associated with the molecular z-axis and smaller with the perpendicular orientations. Furthermore, as we show in the Supporting Information (Figure S8), the enhancing effect of the scavenging reaction is realized independent of the protonation state of the flavin; FADH[•] and FAD^{•-} give rise to comparable enhancements of the reaction anisotropy. Figure 5 provides a tentative reaction scheme uniting the proposed FADH[•]/O₂^{•-} pathways with radical scavenging. If spin relaxation in the superoxide anion proceeds on the time scale of hundreds of nanoseconds or faster, this scheme predicts a broad radio frequency magnetic field response similar to that described in⁶¹⁻⁶².

Note in passing that, as an alternative to the scavenged FADH[•]/O₂^{•-}, a magnetosensitive three-spin system could also result from flavin semiquinone and molecular oxygen, a triplet molecule, forming an f-pair in the presence of a suitable C[•]. This radical-triplet-radical system is, however, beyond the scope of this paper, which centres on three-radical systems.

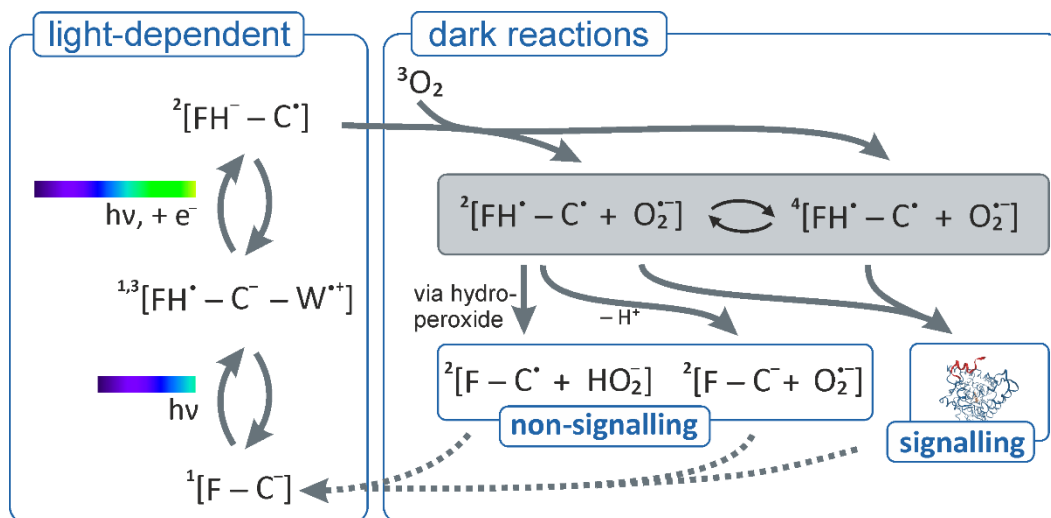


Figure 5: A tentative reaction scheme of a RP-based magnetic compass involving dark-state reoxidation of the fully reduced FADH⁻, the superoxide radical anion (O₂^{•-}) and radical scavenging to avoid the detriment of fast spin relaxation associated with the latter. The spin-correlated FADH[•]/O₂^{•-}-RP is formed in a dark-state reaction from the fully reduced flavin, FADH⁻, and dioxygen. Due to the ³Σ ground state of O₂, this RP is generated exclusively in a (local) triplet state, which corresponds to both doublet and quartet states in the combined system including the initially uncorrelated radical scavenger. The doublet and quartet states interconvert via hyperfine interactions in FADH[•] and C[•] and the Zeeman interactions of all radicals. The MFE arises from the competition between the regeneration of the fully oxidised FAD and the spin-independent formation of the signalling state. Here, we have assumed that the singlet recombination of the FADH[•]/O₂^{•-}-RP produces hydrogen peroxide (H₂O₂), possibly via the C4a-hydroperoxy-flavin, and that C[•] reoxidizes FADH[•] to FAD.⁶⁹ Both assumptions are not critical as long as the products of these spin-selective reactions are disparate from the signalling state. Note that the flavin/tryptophan RP intermediate produced in the light-activation step is likely to be magnetosensitive as well. For the photoreduction steps, the spectral ranges of the light inducing these reactions is schematically shown. The drawn spectra are based on the light-dependence of magnetoreception in birds; for other species the spectral fingerprint may differ, in particular for the second photoreduction step.^{6, 18} We have also assumed that the scavenger radical C[•] is produced in the course of the photoreduction. It could be an oxidised electroactive residue within the protein. Details are discussed in the main text.

Requirements for a hypothetical scavenging-enhanced FADH[•]/O₂^{•-} model

Despite the speculative nature of the proposed scheme as summarized in Figure 5, we do see virtue in discussing pertinent points in order to reveal requirements and

limitations. At the current stage we can only guess as to the identity of C^{\bullet} , which for the $O_2^{\bullet-}$ -containing radicals will have to react with $A^{\bullet-}$, the flavin radical $FADH^{\bullet}$. In principle, this presumably light-independent reaction could involve the reduction, oxidation or any chemical transformation of $A^{\bullet-}$ yielding diamagnetic products. In a cyclic reaction scheme, the latter can always be interpreted as, possibly elaborate, redox-reactions and we will, thus, focus on reduction and oxidation. A reductive scavenging reaction of the semiquinone (i.e. one that transforms $FADH^{\bullet}$ to $FADH^-$) appears unlikely, because it would be redundant to the photochemical reduction, which has been established *in vivo* (e.g. for Cry1a in pigeons¹⁹ and algal cryptochromes⁷⁰) and *in vitro* (e.g. for cryptochrome 1a from the migratory garden warbler⁷¹) and is a central feature of the $FADH^{\bullet}/O_2^{\bullet-}$ hypothesis. The oxidative scavenging of $FADH^{\bullet}$ could be achieved by a multitude of radicals with spin relaxation times comparable to or slower than that of $A^{\bullet-}$. This requirement likely precludes most transition metal compounds and other fast relaxing species such as NO^{\bullet} , HO^{\bullet} or a second $O_2^{\bullet-}$ to act as C^{\bullet} . On the other hand, the radicals derived from tryptophan, tyrosine and most radical scavengers are entirely adequate. It is not unconceivable that the two oxidation equivalents afforded by the photoreduction of FAD to $FADH^-$ are used to generate the radical scavenger in the first place. This would require that the primary oxidation products of the photoinduced forward reaction, e.g. surface exposed tryptophan radicals of the cryptochrome, are stabilized until the magnetoreception process is eventually triggered by reaction of the fully reduced $FADH^-$ with dioxygen. The radical stabilization could involve the deprotonation of the tryptophan radical cation, electron transfer to a tyrosine (in combination with deprotonation), or reaction with an external reactant such as ascorbic acid, tocopherol or ubiquinone (but excluding thiols due to faster spin relaxation) to yield more stable radicals. The stabilization will have to be provided in the presence of $FADH^-$. This could involve conformational changes and/or be attributed to the large exergonicity of the charge recombination (of $FADH^-$ and the scavenger radical), which would slow down the electron transfer as a consequence of the Marcus inverted region. Based on the results in ref¹⁷, lifetimes of the so-stabilized C^{\bullet} of at least ~ 100 ms are necessary. Any spin correlation initially generated in the radical formation will certainly have decayed during this time due to spin relaxation. Note furthermore that many *in vitro* studies of cryptochromes have indeed implicated comparably long-lived tyrosine radicals: $TyrO^{\bullet}$ was identified as a successor of Trp^{\bullet} in the photoactivation of cryptochrome 1a of the garden warbler (lifetime: 14 ms),⁷¹ cryptochrome 1 from *Arabidopsis thaliana* (two populations with lifetimes of 5 and > 100 ms),⁷² and a cryptochrome from *Chlamydomonas reinhardtii* (lifetime: 26 ms).⁷³ Interestingly, in *C. reinhardtii* a tyrosine extending the tryptophan triad appears to be essential for the photoreduction to yield the fully reduced $FADH^-$.⁷³ In unrelated proteins, significantly longer lived tyrosine and tryptophan radicals have been observed (e.g. ⁷⁴ describes tryptophan radicals that persistent for minutes), suggesting that in principle the radical lifetime could be sufficient for the envisaged role as scavenger. The hypothesis that C^{\bullet} might be generated in the photoreduction of FAD could also explain why the resting state contains the fully oxidized FAD (instead of e.g. the semiquinone) and why the photoreduction of FAD

is preferred over the dark-state chemical reduction (which is realized in many flavoproteins such as glucose oxidase).⁶⁷

A second requirement is that the reaction product of the scavenging process is distinct from the pathway giving rise to signalling. In Figure 5, we have assumed that the signalling state derives from FADH[•]/C[•] (with O₂^{•-} possibly escaped into the bulk by diffusion). A conformational change would have to occur in order to distinguish this state from the products of the spin-selective pathways. This could in principle ensue along the lines of activation of the cryptochrome in *D. melanogaster*, for which the formation of the flavin semiquinone triggers a structural rearrangement of the C-terminal tail.⁷⁵ However, any signalling mechanism emanating from the FADH[•]-state is compatible with the scheme. It is imaginable that the conformationally stabilized FADH[•] is eventually photoreduced (e.g. under green light) to regenerate FADH⁻, the putative signalling state suggested in ¹⁹. A magnetic field sensitivity of the FADH⁻-population could also derive from reversibility of the initial oxidation reaction of FADH⁻ and O₂ (as suggested in ³⁴; however experimental studies of the reoxidation do not seem to support reversibility on this stage, at least in a plant cryptochrome ^{23, 76}) or dark reactions generating the fully reduced form such as disproportionation reactions. The messenger could even be O₂^{•-} provided that it is released at different rates/yields from the signalling and scavenged state, as discussed in refs ^{56, 77-78}.

A third limitation concerns the distance of C[•] to the FADH[•]-centre, which for a direct through-protein electron transfer must not exceed 15 Å (edge-to-edge; estimated based on the Moser-Dutton ruler assuming a rate constant of 10⁶ s⁻¹ in the activation-less Marcus limit; more efficient through-bond coupling networks may exist) for the radical scavenging to have an enhancing effect. Using the cryptochrome from *D. melanogaster* (PDB ID: 4GU5) as a representative model (the crystal structures of the bird cryptochromes have not yet been resolved), 11 tryptophans and 7 tyrosines (3 with adjacent histidines) fall within this margin.⁷⁹⁻⁸⁰ It is interesting to note that by triggering the reaction with oxygen in the dark, all 3 radicals are likely well aligned to engage in the amplification process. For the earlier model involving the photogenerated RP FAD^{•-}/W^{•+}, this advantage could likely only be realized if the external C[•] is bound to the cryptochrome, e.g. through a binding partner. One might thus speculate that this difference has provided an evolutionary driver in favour of the more complicated O₂^{•-}-pathway, which on the first glance does not seem to offer any advantages (besides compass orientation under short-term exposure to green light or darkness) and might even appear wasteful by requiring two photons instead of only one.

Magnetosensation in fruit flies

Magnetosensation has also been established in fruit flies. In this context, it is interesting to note that the 'phase' of the MFE observed in neuronal firing and behavioural experiments in *D. melanogaster* suggests a triplet-born RP (in the conventional RP model), if we assume that the effects reflect the concentration of the flavin radical.^{56, 81-83} This also applies if we adopt a signalling pathway involving reoxidation of FAD^{•-} by molecular oxygen, O₂^{•-} as mediator, and the interaction with potassium channels through the NADPH-dependent Hyperkinetic subunit, as suggested in ref ⁵⁶. The observed phase is also compatible with the mechanism of

radical scavenging suggested here, for which the phase of the effect intrinsically corresponds to that of a triplet-born RP in the conventional scheme. Clearly, the mechanism suggested in Figure 5 also requires that the fully reduced state can be attained in a photochemical reduction process. For the cryptochrome form *D. melanogaster*, so far only the chemical reduction has been described *in vitro*.⁷⁵ However, some mutants are susceptible to fast and complete photoreduction, even though the wild type protein adopts a two-state photocycle, with FAD^{•-} as the signalling and FAD as the resting state.⁸⁴⁻⁸⁵ Likewise, a single amino acid mutation can increase the efficiency of the photoreduction to the fully reduced redox state in Arabidopsis cryptochrome 1, thereby effectively incurring photolyase activity to the protein.⁸⁶

Conclusions

Radical scavenging can drastically boost the performance of the quantum magnetic compass as assessed from the absolute and relative anisotropy, Δ_S and Γ_S , respectively. As for the classical RP model, in most circumstances the effect is attenuated by noisy environments as a result of decoherence and spin relaxation. Yet, in the presence of radical scavenging markedly faster spin relaxation rates can be accommodated to achieve the necessary anisotropy than for the conventional RP model. Surprisingly, the enhancing effect of radical scavenging is not degraded by fast spin relaxation in the un-scavenged radical of the original pair, B^{•+}. This tremendously broadens the scope of the RPM to include swiftly relaxing species such as transition metal compounds, superoxide, nitroxide, etc. This is noteworthy because these species are often involved/generated in thermal electron transfer reactions, for which, in stark contrast to the orthodoxy of the field, new avenues to MFEs in weak magnetic fields emerge. Even more surprisingly, the performance of the magnetic compass was found to be enhanced by fast relaxation in B^{•+}.

We have discussed the applicability of the scavenging amplification scheme to a postulated FADH[•]/O₂^{•-}-based magnetic compass, for which some evidence has recently accumulated. While the isolated FADH[•]/O₂^{•-} RP can hardly be a suitable basis of a compass sense due to fast spin relaxation in O₂^{•-}, in combination with radical scavenging of the flavin semiquinone a formidable compass sensor could be realized. This compass would surpass the classical model even in the ideal of no relaxation by an order of magnitude in the relative anisotropy and would even profit from the fast spin relaxation in O₂^{•-}. Obviously, the suggested radical scavenging-enhanced mechanism is subject to prerequisites and constraints, which we have discussed in some depth. Our naïve model is based on an isolated cryptochrome for which the oxidative radical scavenger, C[•], is produced in the course of the photoreduction of FAD. This model could be tested *in vitro* by recording the MFE on the semiquinone produced in the reoxidation of FADH⁻ immediately (within the lifetime of the oxidized residues, i.e. hundreds of milliseconds) following its generation by photoreduction. Furthermore, behavioural studies of the kind introduced in ref ¹⁷ could be used to elucidate additional details of the mechanism. In view of the proposed model, these

experiments could be extended to involve alternating light and magnetic field exposure disrupted by periods of darkness/red light exposure in the absence of the magnetic field. Varying the length of this delay period, could reveal whether photogenerated scavenging radicals are indeed involved. If true, the magnetosensation would be impaired by too long delays on the order of hundreds of milliseconds. While speculative, our analysis imparts credible feasibility to $O_2^{\bullet-}$ -based models in magnetoreception and MFEs. It is hoped that our insights can aid the identification of the magnetically sensitive RP reaction(s) in cryptochromes.

Supporting Information. Used hyperfine parameters, plots of Δ_s , reaction anisotropies of triplet-born $[FAD^{\bullet-} Z^{\bullet}]$ and $[FADH^{\bullet} Z^{\bullet}]$ radical pairs subject to radical scavenging, additional data on the effect of relaxation in various combinations of radicals of the spin triad, $\Gamma_s(k_c=51.8 \mu s^{-1})/\Gamma_s(k_c=0)$ as a function of γ , and an overlay of the data from Figure 2a and 2b.

Acknowledgements

The author is indebted to Prof. Peter Hore (University of Oxford) for continuous support and many stimulating discussions. This work was partly conceived during the author affiliation with the Hore group at the University of Oxford, where it was supported by the European Research Council (under the European Union's 7th Framework Programme, FP7/2007-2013/ERC Grant Agreement No. 340451) and the Air Force Office of Scientific Research (Air Force Materiel Command, USAF award no. FA9550-14-1-0095). The author thanks Dr. Alex Jones (University of Manchester) for discussion of the scavenging mechanism in the context of magnetic field effects in *D. melanogaster*. The image of the robin used in the TOC graphic is extracted from a photograph by Artur Rydzewski, which is licensed under a Creative Commons Attribution 4.0 International License.

References

1. Schulten, K.; Swenberg, C. E.; Weller, A., A biomagnetic sensory mechanism based on magnetic field modulated coherent electron spin motion. *Z. Phys. Chem.* **1978**, *111*, 1-5.
2. Ritz, T.; Adem, S.; Schulten, K., A model for photoreceptor-based magnetoreception in birds. *Biophys. J.* **2000**, *78*, 707-718.
3. Chaves, I.; Pokorny, R.; Byrdin, M.; Hoang, N.; Ritz, T.; Brettel, K.; Essen, L. O.; van der Horst, G. T.; Batschauer, A.; Ahmad, M., The cryptochromes: blue light photoreceptors in plants and animals. *Annu. Rev. Plant Biol.* **2011**, *62*, 335-64.
4. Hore, P. J.; Mouritsen, H., The radical-pair mechanism of magnetoreception. *Annu. Rev. Biophys.* **2016**, *45*, 299-344.
5. Wiltschko, R.; Wiltschko, W., Sensing magnetic directions in birds: radical pair processes involving cryptochrome. *Biosensors* **2014**, *4*, 221-42.
6. Phillips, J. B.; Jorge, P. E.; Muheim, R., Light-dependent magnetic compass orientation in amphibians and insects: candidate receptors and candidate molecular mechanisms. *J. R. Soc., Interface* **2010**, *7*, S241-S256.

7. Phillips, J. B.; Muheim, R.; Jorge, P. E., A behavioral perspective on the biophysics of the light-dependent magnetic compass: a link between directional and spatial perception? *J. Exp. Biol.* **2010**, *213*, 3247-3255.
8. Wiltschko, R.; Wiltschko, W., *Magnetic Orientation in Animals*. Springer: Berlin, New York, 1995; p xvii, 297 p.
9. Wiltschko, R.; Wiltschko, W., Magnetoreception. In *Sensing in Nature*, López-Larrea, C., Ed. Springer: New York, 2012; Vol. 739, pp 126-141.
10. Liedvogel, M.; Mouritsen, H., Cryptochromes - a potential magnetoreceptor: what do we know and what do we want to know? *J. R. Soc., Interface* **2010**, *7*, S147-S162.
11. Rodgers, C. T.; Hore, P. J., Chemical magnetoreception in birds: The radical pair mechanism. *Proc. Natl. Acad. Sci. U. S. A.* **2009**, *106*, 353-360.
12. Steiner, U. E.; Ulrich, T., Magnetic-field effects in chemical-kinetics and related phenomena. *Chem. Rev.* **1989**, *89*, 51-147.
13. Salikhov, K. M.; Molin, I. U. N.; Buchachenko, A. L., *Spin polarization and magnetic effects in radical reactions*. Elsevier Amsterdam, 1984.
14. Maeda, K.; Robinson, A. J.; Henbest, K. B.; Hogben, H. J.; Biskup, T.; Ahmad, M.; Schleicher, E.; Weber, S.; Timmel, C. R.; Hore, P. J., Magnetically sensitive light-induced reactions in cryptochrome are consistent with its proposed role as a magnetoreceptor. *Proc. Natl. Acad. Sci. U. S. A.* **2012**, *109*, 4774-4779.
15. Sheppard, D. M. W.; Li, J.; Henbest, K. B.; Neil, S. R. T.; Maeda, K.; Storey, J.; Schleicher, E.; Biskup, T.; Rodriguez, R.; Weber, S.; Hore, P. J.; Timmel, C. R.; Mackenzie, S. R., Millitesla magnetic field effects on the photocycle of an animal cryptochrome. *Sci. Rep.* **2017**, *7*, 42228.
16. Weber, S.; Biskup, T.; Okafuji, A.; Marino, A. R.; Berthold, T.; Link, G.; Hitomi, K.; Getzoff, E. D.; Schleicher, E.; Norris, J. R., Origin of light-induced spin-correlated radical pairs in cryptochrome. *J. Phys. Chem. B* **2010**, *114*, 14745-14754.
17. Wiltschko, R.; Ahmad, M.; Nießner, C.; Gehring, D.; Wiltschko, W., Light-dependent magnetoreception in birds: The crucial step occurs in the dark. *J. R. Soc., Interface* **2016**, *13*, 20151010.
18. Wiltschko, R.; Stapput, K.; Thalau, P.; Wiltschko, W., Directional orientation of birds by the magnetic field under different light conditions. *J. R. Soc., Interface* **2010**, *7 Suppl 2*, S163-77.
19. Nießner, C.; Denzau, S.; Stapput, K.; Ahmad, M.; Peichl, L.; Wiltschko, W.; Wiltschko, R., Magnetoreception: activated cryptochrome 1a concurs with magnetic orientation in birds. *J. R. Soc., Interface* **2013**, *10*, 20130638.
20. Nießner, C.; Denzau, S.; Peichl, L.; Wiltschko, W.; Wiltschko, R., Magnetoreception in birds: I. Immunohistochemical studies concerning the cryptochrome cycle. *J. Exp. Biol.* **2014**, *217*, 4221-4.
21. Wiltschko, R.; Gehring, D.; Denzau, S.; Nießner, C.; Wiltschko, W., Magnetoreception in birds: II. Behavioural experiments concerning the cryptochrome cycle. *J. Exp. Biol.* **2014**, *217*, 4225-8.
22. Ritz, T.; Wiltschko, R.; Hore, P. J.; Rodgers, C. T.; Stapput, K.; Thalau, P.; Timmel, C. R.; Wiltschko, W., Magnetic compass of birds is based on a molecule with optimal directional sensitivity. *Biophys. J.* **2009**, *96*, 3451-3457.
23. Müller, P.; Ahmad, M., Light-activated cryptochrome reacts with molecular oxygen to form a flavin-superoxide radical pair consistent with magnetoreception. *J. Biol. Chem.* **2011**, *286*, 21033-40.

24. Kattnig, D. R.; Hore, P. J., The sensitivity of a radical pair compass magnetoreceptor can be significantly amplified by radical scavengers. *Sci. Rep.* **2017**, *7*, 11640.
25. Hiscock, H. G.; Kattnig, D. R.; Manolopoulos, D. E.; Hore, P. J., Floquet theory of radical pairs in radiofrequency magnetic fields. *J. Chem. Phys.* **2016**, *145*, 124117.
26. Hiscock, H. G.; Worster, S.; Kattnig, D. R.; Steers, C.; Jin, Y.; Manolopoulos, D. E.; Mouritsen, H.; Hore, P. J., The quantum needle of the avian magnetic compass. *Proc. Natl. Acad. Sci. U. S. A.* **2016**, *113*, 4634-4639.
27. Kattnig, D. R.; Solov'yov, I. A.; Hore, P. J., Electron spin relaxation in cryptochrome-based magnetoreception. *Phys. Chem. Chem. Phys.* **2016**, *18*, 12443-12456.
28. Kattnig, D. R.; Sowa, J. K.; Solov'yov, I. A.; Hore, P. J., Electron spin relaxation can enhance the performance of a cryptochrome-based magnetic compass sensor. *New J. Phys.* **2016**, *18*, 063007.
29. Lee, A. A.; Lau, J. C. S.; Hogben, H. J.; Biskup, T.; Kattnig, D. R.; Hore, P. J., Alternative radical pairs for cryptochrome-based magnetoreception. *J. R. Soc., Interface* **2014**, *11*, 20131063.
30. Gauger, E. M.; Rieper, E.; Morton, J. J. L.; Benjamin, S. C.; Vedral, V., Sustained quantum coherence and entanglement in the avian compass. *Phys. Rev. Lett.* **2011**, *106*, 040503.
31. Cai, J. M.; Guerreschi, G. G.; Briegel, H. J., Quantum control and entanglement in a chemical compass. *Phys. Rev. Lett.* **2010**, *104*, 220502.
32. Kavokin, K. V., The puzzle of magnetic resonance effect on the magnetic compass of migratory birds. *Bioelectromagnetics* **2009**, *30*, 402-10.
33. Zhang, Y. T.; Berman, G. P.; Kais, S., The radical pair mechanism and the avian chemical compass: Quantum coherence and entanglement. *Int. J. Quantum Chem.* **2015**, *115*, 1327-1341.
34. Hogben, H. J.; Efimova, O.; Wagner-Rundell, N.; Timmel, C. R.; Hore, P. J., Possible involvement of superoxide and dioxygen with cryptochrome in avian magnetoreception: Origin of Zeeman resonances observed by *in vivo* EPR spectroscopy. *Chem. Phys. Lett.* **2009**, *480*, 118-122.
35. Kattnig, D. R.; Evans, E. W.; Dejean, V.; Dodson, C. A.; Wallace, M. I.; Mackenzie, S. R.; Timmel, C. R.; Hore, P. J., Chemical amplification of magnetic field effects relevant to avian magnetoreception. *Nat. Chem.* **2016**, *8*, 384-391.
36. Letuta, A. S.; Berdinskii, V. L., Chemical Zeno effect - A new mechanism of spin catalysis in radical triads. *Dokl. Phys. Chem.* **2015**, *463*, 179-181.
37. Cailliez, F.; Müller, P.; Firmino, T.; Pernot, P.; de la Lande, A., Energetics of photoinduced charge migration within the tryptophan tetrad of an animal (6-4) photolyase. *J. Am. Chem. Soc.* **2016**, *138*, 1904-1915.
38. Müller, P.; Yamamoto, J.; Martin, R.; Iwai, S.; Brettel, K., Discovery and functional analysis of a 4th electron-transferring tryptophan conserved exclusively in animal cryptochromes and (6-4) photolyases. *Chem. Commun.* **2015**, *51*, 15502-15505.
39. Efimova, O.; Hore, P. J., Role of exchange and dipolar interactions in the radical pair model of the avian magnetic compass. *Biophys. J.* **2008**, *94*, 1565-1574.
40. Lukzen, N. N.; Usov, O. M.; Molin, Y. N., Magnetic field effects in the recombination fluorescence of a three-spin radical ion/biradical ion system. *Phys. Chem. Chem. Phys.* **2002**, *4*, 5249-5258.

41. Sviridenko, F. B.; Stass, D. V.; Kobzeva, T. V.; Tretyakov, E. V.; Klyatskaya, S. V.; Mshvidobadze, E. V.; Vasilevsky, S. F.; Molin, Y. N., Optically detected ESR and low magnetic field signals from spin triads: 2-imidazoline-1-oxyl derivatives in X-irradiated alkane liquids as a method to study three-spin systems. *J. Am. Chem. Soc.* **2004**, *126*, 2807-2819.
42. Buchachenko, A. L.; Berdinsky, V. L., Spin catalysis of chemical reactions. *J. Phys. Chem.* **1996**, *100*, 18292-18299.
43. Magin, I. M.; Purtov, P. A.; Kruppa, A. I.; Leshina, T. V., Peculiarities of magnetic and spin effects in a biradical/stable radical complex (three-spin system). Theory and comparison with experiment. *J. Phys. Chem. A* **2005**, *109*, 7396-7401.
44. Pedersen, J. B.; Nielsen, C.; Solov'yov, I. A., Multiscale description of avian migration: from chemical compass to behaviour modeling. *Sci. Rep.* **2016**, *6*, 36709.
45. Dellis, A. T.; Kominis, I. K., The quantum Zeno effect immunizes the avian compass against the deleterious effects of exchange and dipolar interactions. *BioSystems* **2012**, *107*, 153-157.
46. Cai, J. M.; Caruso, F.; Plenio, M. B., Quantum limits for the magnetic sensitivity of a chemical compass. *Phys. Rev. A* **2012**, *85*, 040304(R).
47. Carrillo, A.; Cornelio, M. F.; de Oliveira, M. C., Environment-induced anisotropy and sensitivity of the radical pair mechanism in the avian compass. *Phys. Rev. E* **2015**, *92*, 012720.
48. Haberkorn, R., Density matrix description of spin-selective radical pair reactions. *Mol. Phys.* **1976**, *32*, 1491-1493.
49. Cai, J. M.; Plenio, M. B., Chemical compass model for avian magnetoreception as a quantum coherent device. *Phys. Rev. Lett.* **2013**, *111*, 230503.
50. Xu, B. M.; Zou, J.; Li, H.; Li, J. G.; Shao, B., Effect of radio frequency fields on the radical pair magnetoreception model. *Phys. Rev. E* **2014**, *90*, 042711.
51. Evans, E. W.; Kattnig, D. R.; Henbest, K. B.; Hore, P. J.; Mackenzie, S. R.; Timmel, C. R., Sub-millitesla magnetic field effects on the recombination reaction of flavin and ascorbic acid radicals. *J. Chem. Phys.* **2016**, *145*, 085101.
52. Henbest, K. B.; Maeda, K.; Hore, P. J.; Joshi, M.; Bacher, A.; Bittl, R.; Weber, S.; Timmel, C. R.; Schleicher, E., Magnetic-field effect on the photoactivation reaction of Escherichia coli DNA photolyase. *Proc. Natl. Acad. Sci. U. S. A.* **2008**, *105*, 14395-14399.
53. Muheim, R.; Backman, J.; Akesson, S., Magnetic compass orientation in European robins is dependent on both wavelength and intensity of light. *J. Exp. Biol.* **2002**, *205*, 3845-3856.
54. Wiltschko, W.; Wiltschko, R., Light-dependent magnetoreception in birds: The behaviour of European robins, *Erithacus rubecula*, under monochromatic light of various wavelengths and intensities. *J. Exp. Biol.* **2001**, *204*, 3295-3302.
55. Gegear, R. J.; Foley, L. E.; Casselman, A.; Reppert, S. M., Animal cryptochromes mediate magnetoreception by an unconventional photochemical mechanism. *Nature* **2010**, *463*, 804-U114.
56. Giachello, C. N. G.; Scrutton, N. S.; Jones, A. R.; Baines, R. A., Magnetic fields modulate blue-light-dependent regulation of neuronal firing by cryptochrome. *J. Neurosci.* **2016**, *36*, 10742-10749.
57. Engelhard, C.; Wang, X. C.; Robles, D.; Moldt, J.; Essen, L. O.; Batschauer, A.; Bittl, R.; Ahmad, M., Cellular metabolites enhance the light sensitivity of

- Arabidopsis* cryptochrome through alternate electron transfer pathways. *Plant Cell* **2014**, *26*, 4519-4531.
58. Biskup, T.; Hitomi, K.; Getzoff, E. D.; Krapf, S.; Koslowski, T.; Schleicher, E.; Weber, S., Unexpected electron transfer in cryptochrome identified by time-resolved epr spectroscopy. *Angew. Chem. Int. Ed.* **2011**, *50*, 12647-12651.
59. Kavokin, K.; Chernetsov, N.; Pakhomov, A.; Bojarinova, J.; Kobylkov, D.; Namozov, B., Magnetic orientation of garden warblers (*Sylvia borin*) under 1.4 MHz radiofrequency magnetic field. *J. R. Soc., Interface* **2014**, *11*, 20140451.
60. Wiltschko, R.; Thalau, P.; Gehring, D.; Nießner, C.; Ritz, T.; Wiltschko, W., Magnetoreception in birds: The effect of radio-frequency fields. *J. R. Soc., Interface* **2015**, *12*, 20141103.
61. Schwarze, S.; Schneider, N. L.; Reichl, T.; Dreyer, D.; Lefeldt, N.; Engels, S.; Baker, N.; Hore, P. J.; Mouritsen, H., Weak broadband electromagnetic fields are more disruptive to magnetic compass orientation in a night-migratory songbird (*Erithacus rubecula*) than strong narrow-band fields. *Front. Behav. Neurosci.* **2016**, *10*, 55.
62. Engels, S.; Schneider, N. L.; Lefeldt, N.; Hein, C. M.; Zapka, M.; Michalik, A.; Elbers, D.; Kittel, A.; Hore, P. J.; Mouritsen, H., Anthropogenic electromagnetic noise disrupts magnetic compass orientation in a migratory bird. *Nature* **2014**, *509*, 353–356.
63. Hiscock, H. G.; Mouritsen, H.; Manolopoulos, D. E.; Hore, P. J., Disruption of magnetic compass orientation in migratory birds by radiofrequency electromagnetic fields. *Biophys. J.* **2017**, *113*, 1475-1484
64. Karogodina, T. Y.; Dranov, I. G.; Sergeeva, S. V.; Stass, D. V.; Steiner, U. E., Kinetic magnetic-field effect involving the small biologically relevant inorganic radicals NO and O₂(-). *ChemPhysChem* **2011**, *12*, 1714-28.
65. Kuimova, M. K.; Yahioglu, G.; Levitt, J. A.; Suhling, K., Molecular rotor measures viscosity of live cells via fluorescence lifetime imaging. *J. Am. Chem. Soc.* **2008**, *130*, 6672–6673.
66. Ritz, T.; Thalau, P.; Phillips, J. B.; Wiltschko, R.; Wiltschko, W., Resonance effects indicate a radical-pair mechanism for avian magnetic compass. *Nature* **2004**, *429*, 177-180.
67. Messiha, H. L.; Wongnate, T.; Chaiyen, P.; Jones, A. R.; Scrutton, N. S., Magnetic field effects as a result of the radical pair mechanism are unlikely in redox enzymes. *J. R. Soc., Interface* **2015**, *12*, 20141155.
68. Solov'yov, I. A.; Schulten, K., Magnetoreception through Cryptochrome May Involve Superoxide. *Biophys. J.* **2009**, *96*, 4804-4813.
69. Massey, V., Activation of molecular-oxygen by flavins and flavoproteins. *J. Biol. Chem.* **1994**, *269*, 22459-22462.
70. Beel, B.; Prager, K.; Spexard, M.; Sasso, S.; Weiss, D.; Müller, N.; Heinnickel, M.; Dewez, D.; Ikoma, D.; Grossman, A. R.; Kottke, T.; Mittag, M., A flavin binding cryptochrome photoreceptor responds to both blue and red light in *Chlamydomonas reinhardtii*. *Plant Cell* **2012**, *24*, 2992-3008.
71. Liedvogel, M.; Maeda, K.; Henbest, K.; Schleicher, E.; Simon, T.; Timmel, C. R.; Hore, P. J.; Mouritsen, H., Chemical magnetoreception: Bird cryptochrome 1a is excited by blue light and forms long-lived radical-pairs. *PLoS One* **2007**, *2*, e1106.
72. Baldissera, G.; Byrdin, M.; Ahmad, M.; Brettel, K., Light-induced electron transfer in a cryptochrome blue-light photoreceptor. *Nat. Struct. Biol.* **2003**, *10*, 489-490.

73. Nohr, D.; Franz, S.; Rodriguez, R.; Paulus, B.; Essen, L. O.; Weber, S.; Schleicher, E., Extended electron-transfer in animal cryptochromes mediated by a tetrad of aromatic amino acids. *Biophys. J.* **2016**, *111*, 301-311.
74. Bleifuss, G.; Kolberg, M.; Potsch, S.; Hofbauer, W.; Bittl, R.; Lubitz, W.; Graslund, A.; Lassmann, G.; Lenzian, F., Tryptophan and tyrosine radicals in ribonucleotide reductase: A comparative high-field EPR study at 94 GHz. *Biochem.* **2001**, *40*, 15362-15368.
75. Vaidya, A. T.; Top, D.; Manahan, C. C.; Tokuda, J. M.; Zhang, S.; Pollack, L.; Young, M. W.; Crane, B. R., Flavin reduction activates *Drosophila* cryptochrome. *Proc. Natl. Acad. Sci. U. S. A.* **2013**, *110*, 20455-20460.
76. van Wilderen, L. J.; Silkstone, G.; Mason, M.; van Thor, J. J.; Wilson, M. T., Kinetic studies on the oxidation of semiquinone and hydroquinone forms of *Arabidopsis* cryptochrome by molecular oxygen. *FEBS Open Bio* **2015**, *5*, 885-92.
77. Consentino, L.; Lambert, S.; Martino, C.; Jourdan, N.; Bouchet, P. E.; Witczak, J.; Castello, P.; El-Esawi, M.; Corbineau, F.; d'Harlingue, A.; Ahmad, M., Blue-light dependent reactive oxygen species formation by *Arabidopsis* cryptochrome may define a novel evolutionarily conserved signaling mechanism. *New Phytol.* **2015**, *206*, 1450-1462.
78. Arthaut, L. D.; Jourdan, N.; Mteyrek, A.; Procopio, M.; El-Esawi, M.; d'Harlingue, A.; Bouchet, P. E.; Witczak, J.; Ritz, T.; Klarsfeld, A.; Birman, S.; Usselman, R. J.; Hoecker, U.; Martino, C. F.; Ahmad, M., Blue-light induced accumulation of reactive oxygen species is a consequence of the *Drosophila* cryptochrome photocycle. *PLoS One* **2017**, *12*, e0171836.
79. Zoltowski, B. D.; Vaidya, A. T.; Top, D.; Widom, J.; Young, M. W.; Crane, B. R., Structure of full-length *Drosophila* cryptochrome. *Nature* **2011**, *480*, 396-399.
80. Levy, C.; Zoltowski, B. D.; Jones, A. R.; Vaidya, A. T.; Top, D.; Widom, J.; Young, M. W.; Scrutton, N. S.; Crane, B. R.; Leys, D., Updated structure of *Drosophila* cryptochrome. *Nature* **2013**, *495*, E3-E4.
81. Fedele, G.; Edwards, M. D.; Bhutani, S.; Hares, J. M.; Murbach, M.; Green, E. W.; Dissel, S.; Hastings, M. H.; Rosato, E.; Kyriacou, C. P., Genetic analysis of circadian responses to low frequency electromagnetic fields in *Drosophila melanogaster*. *PLoS Genet.* **2014**, *10*, e1004804.
82. Fedele, G.; Green, E. W.; Rosato, E.; Kyriacou, C. P., An electromagnetic field disrupts negative geotaxis in *Drosophila* via a CRY-dependent pathway. *Nature Communications* **2014**, *5*, 4391.
83. Marley, R.; Giachello, C. N. G.; Scrutton, N. S.; Baines, R. A.; Jones, A. R., Cryptochrome-dependent magnetic field effect on seizure response in *Drosophila* larvae. *Sci. Rep.* **2015**, *4*, 5799.
84. Kao, Y. T.; Tan, C.; Song, S. H.; Ozturk, N.; Li, J.; Wang, L. J.; Sancar, A.; Zhong, D. P., Ultrafast dynamics and anionic active states of the flavin cofactor in cryptochrome and photolyase. *J. Am. Chem. Soc.* **2008**, *130*, 7695-7701.
85. Berndt, A.; Kottke, T.; Breitzkreuz, H.; Dvorsky, R.; Hennig, S.; Alexander, M.; Wolf, E., A novel photoreaction mechanism for the circadian blue light photoreceptor *Drosophila* cryptochrome. *J. Biol. Chem.* **2007**, *282*, 13011-13021.
86. Burney, S.; Wenzel, R.; Kottke, T.; Roussel, T.; Hoang, N.; Bouly, J. P.; Bittl, R.; Heberle, J.; Ahmad, M., Single amino acid substitution reveals latent photolyase activity in *Arabidopsis cry1*. *Angew. Chem. Int. Ed.* **2012**, *51*, 9356-9360.

Supporting Information

Radical-Pair Based Magnetoreception Amplified by Radical Scavenging: Resilience to Spin Relaxation

Daniel R. Kattnig*

University of Exeter, Living Systems Institute and Department of Physics, Stocker Road, Exeter, Devon, EX4 4QD, U.K.

* Author for correspondence: d.r.kattnig@exeter.ac.uk

- Table S1:** Hyperfine parameters.
- Figure S1:** Absolute reaction anisotropy, Δ_s , as a function of k_c or γ of model three-radical system subject to radical scavenging and spin relaxation.
- Figure S2:** Overlay of the data from Figure 2a and 2b.
- Figure S3:** $\Gamma_s(k_c=51.8 \mu\text{s}^{-1})/\Gamma_s(k_c=0)$ as a function of the global spin relaxation rate γ .
- Figure S4:** Dependence of absolute reaction anisotropy on the rate of random-field spin relaxation in chosen parts of model three-radical systems.
- Figure S5:** Anisotropic yields of the signalling state for a model $[\text{FAD}^{\bullet-} \text{W}^{\bullet+}]$ radical pair subject to radical scavenging and spin relaxation affecting chosen radicals.
- Figure S6:** Contour plots of Δ_s as a function of k_c and γ for a model $[\text{FAD}^{\bullet-} \text{W}^{\bullet+}]$ radical pair with spin relaxation in all or individual radicals.
- Figure S7:** Anisotropic yields of the signalling state for a triplet-born $[\text{FAD}^{\bullet-} \text{Z}^{\bullet}]$ radical pair subject to radical scavenging.
- Figure S8:** Anisotropic yields of the signalling state for a triplet-born $[\text{FADH}^{\bullet} \text{Z}^{\bullet}]$ radical pair subject to radical scavenging.

Table S1: Hyperfine parameters of the model systems used in this study. These hyperfine tensors are identical to those used in reference [1]. See [2] for a detailed description of their derivation.

FAD^{•-}	
N5	$A_{N5} = \begin{pmatrix} -2.77 & 0.11 & 0 \\ 0.11 & -2.47 & 0 \\ 0 & 0 & 49.24 \end{pmatrix}$ MHz
N10	$A_{N10} = \begin{pmatrix} -0.53 & -0.13 & 0 \\ -0.13 & -0.55 & 0 \\ 0 & 0 & 16.94 \end{pmatrix}$ MHz
H6	$A_{H6} = \begin{pmatrix} -7.20 & -3.57 & 0 \\ -3.57 & -13.20 & 0 \\ 0 & 0 & -12.15 \end{pmatrix}$ MHz
3 × H8	$A_{H8} = \begin{pmatrix} 12.33 & 0 & 0 \\ 0 & 12.33 & 0 \\ 0 & 0 & 12.33 \end{pmatrix}$ MHz
2 × Hβ	$A_{Hβ} = \begin{pmatrix} 11.41 & 0 & 0 \\ 0 & 11.41 & 0 \\ 0 & 0 & 11.41 \end{pmatrix}$ MHz
Wc^{•+}	
N1	$A_{N10} = \begin{pmatrix} -0.94 & 2.59 & -3.79 \\ 2.59 & 9.26 & -14.90 \\ -3.79 & -14.90 & 18.72 \end{pmatrix}$ MHz

1. D. R. Kattnig and P. J. Hore, *Sci. Rep.*, 2017, **7**, 11640.
2. A. A. Lee, J. C. S. Lau, H. J. Hogben, T. Biskup, D. R. Kattnig and P. J. Hore, *J. R. Soc. Interface*, 2014, **11**, 20131063.

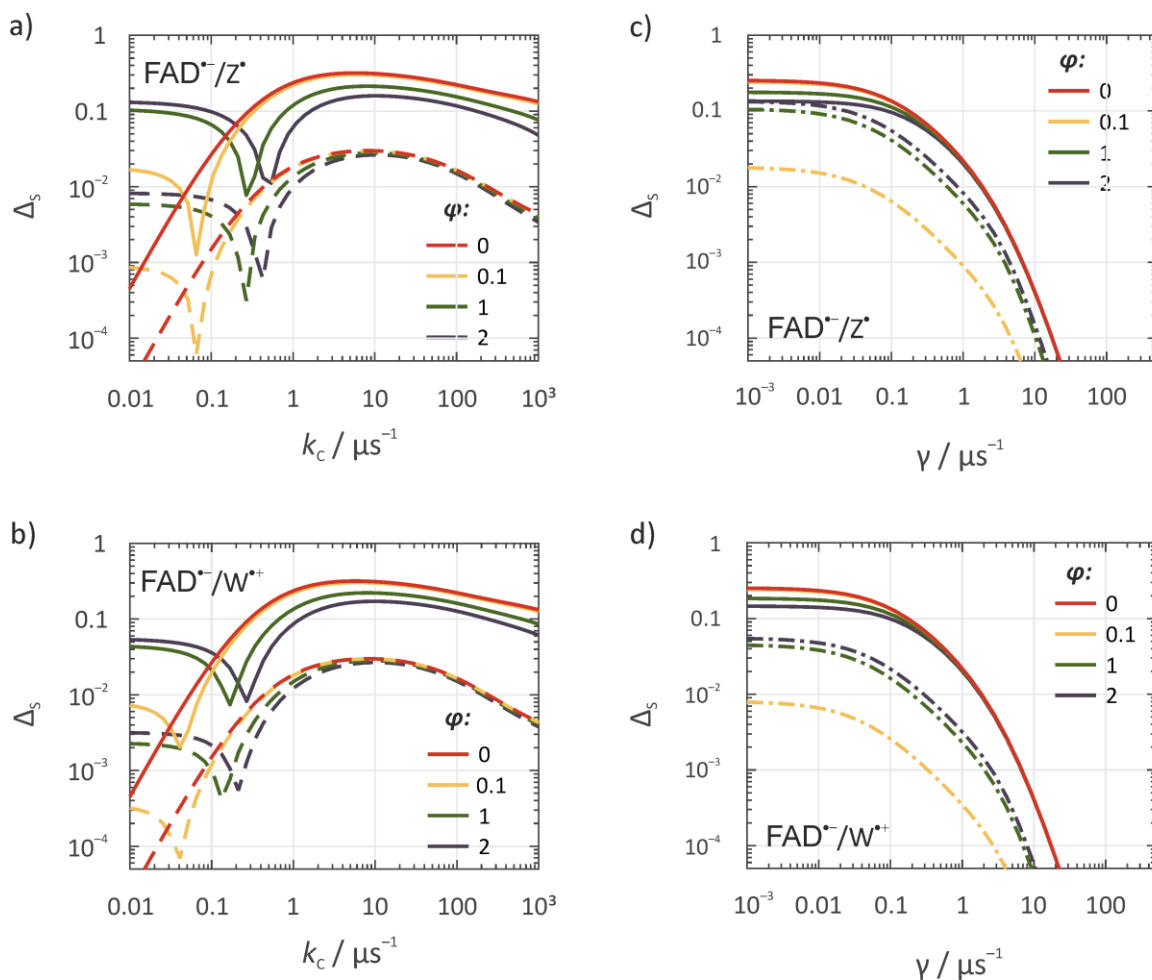


Figure S1: Absolute reaction anisotropy as a function of k_c or γ . Panels *a)* and *b)*: Dependence of Δ_s on k_c in the absence (solid lines) and presence (dashed lines) of spin relaxation with $\gamma = \gamma_A = \gamma_B = \gamma_C = 1 \mu\text{s}^{-1}$ for various $\phi = k_b/k_f$ as encoded by the different colours and summarized in the common legends. Panels *c)* and *d)*: Dependence of Δ_s on $\gamma = \gamma_A = \gamma_B = \gamma_C$ for $k_c = 51.8 \mu\text{s}^{-1}$ (solid lines) and $k_c = 0 \text{ s}^{-1}$ (no scavenging, dashed-dotted lines). All calculations are based on a spin system comprising N5 and N10 of $\text{FAD}^{\bullet-}$ in $\text{A}^{\bullet-}$ and no hyperfine coupled nuclei in C^{\bullet} . For panels *a)* and *c)* no hyperfine coupled nuclei are present in $\text{B}^{\bullet+}$ ($\text{FAD}^{\bullet-}/\text{Z}^{\bullet}$ model); for panels *b)* and *d)* N1 of $\text{W}^{\bullet+}$ has been included ($\text{FAD}^{\bullet-}/\text{W}^{\bullet+}$ model). See Figure 2 of the main manuscript for additional details.

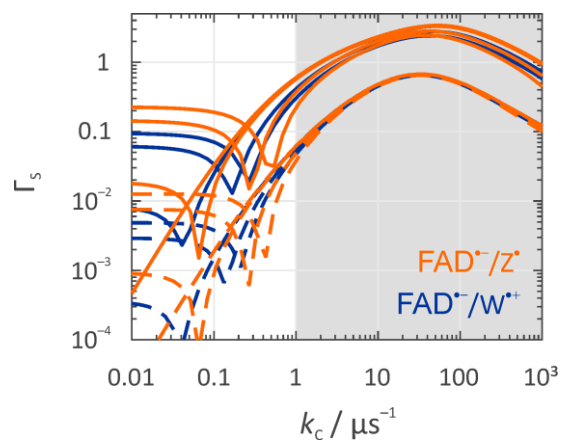


Figure S2: Overlay of the data from Figure 2a and 2b. The plot gives the relative anisotropy as a function of k_c for the $\text{FAD}^{\bullet-}/\text{Z}^{\bullet}$ (orange lines) and the $\text{FAD}^{\bullet-}/\text{W}^{\bullet+}$ (blue lines) model in the absence (solid lines) and presence (dashed lines) of relaxation for four different values of φ . Refer to the caption of Figure 2 for details. Under conditions of significant radical scavenging (region shaded in grey) the relative anisotropies are nearly unaffected by the identity of $\text{B}^{\bullet+}$.

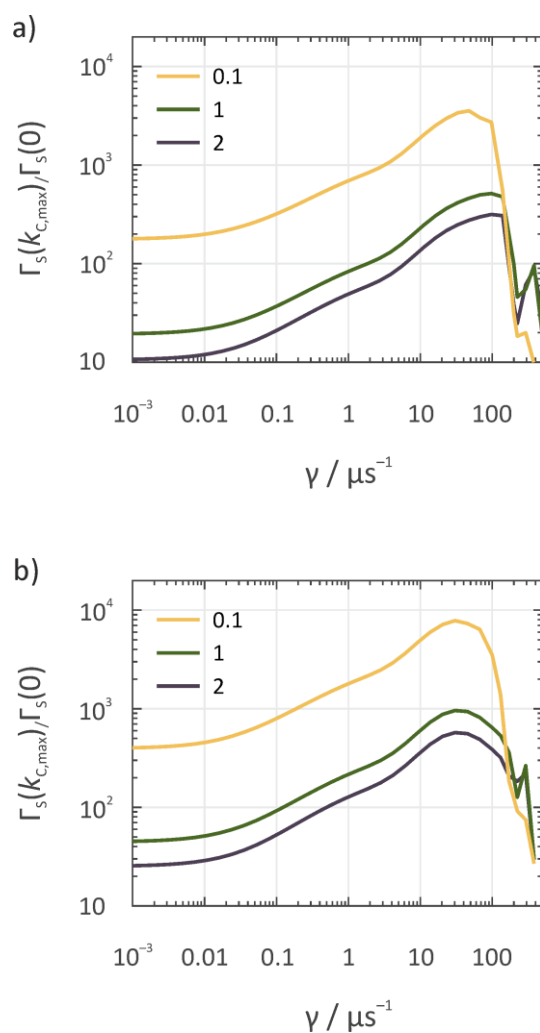


Figure S3: Ratio of the relative anisotropy Γ_s of the signalling state in the presences and absence of radical scavenging, $\Gamma_s(k_c=51.8 \mu s^{-1})/\Gamma_s(k_c=0)$, as a function of the relaxation rate γ for various $\varphi = k_b/k_f$ (as encoded by the different colours and summarized in the legend) for a) the $FAD^{\bullet-}/Z^{\bullet}$ and b) the $FAD^{\bullet-}/W^{\bullet+}$ model. Random field spin relaxation was present in all radicals: $\gamma = \gamma_A = \gamma_B = \gamma_C$. $B_0 = 50 \mu T$ and $k_f = 0.1 \mu s^{-1}$.

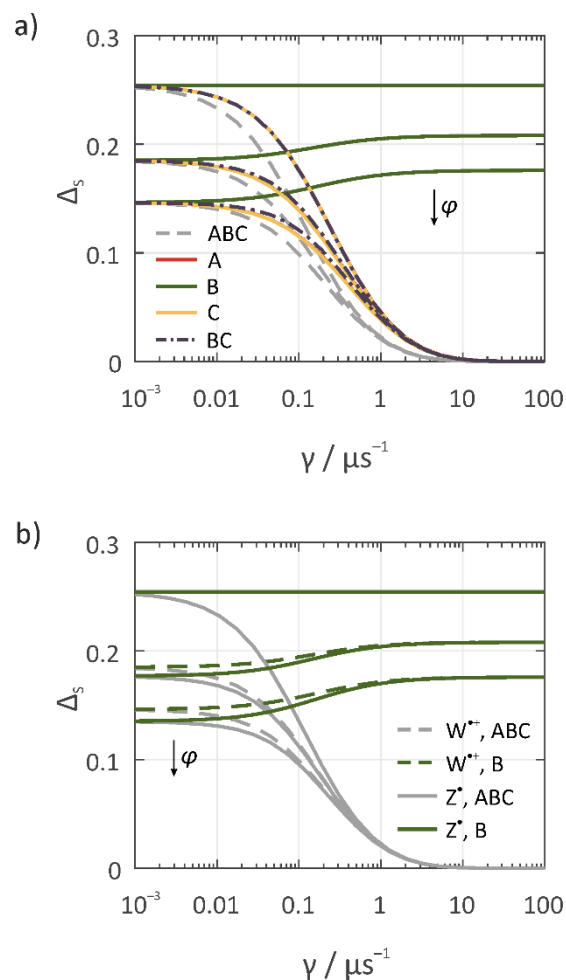


Figure S4: Dependence of Δ_s on the rate of random-field spin relaxation in chosen parts of the three-radical system for $\varphi = k_b/k_f = 0, 1, \text{ and } 2$. Panel *a)* applies to the scavenged $\text{FAD}^{\bullet-}/\text{W}^{\bullet+}$ scenario. In panel *b)* the $\text{FAD}^{\bullet-}/\text{W}^{\bullet+}$ model is compared to the $\text{FAD}^{\bullet-}/\text{Z}^{\bullet}$ model. The legends name the radicals that are impacted by spin relaxation. $k_c = 51.8 \mu\text{s}^{-1}$. Further details are available from the caption of Figure 3 of the main document.

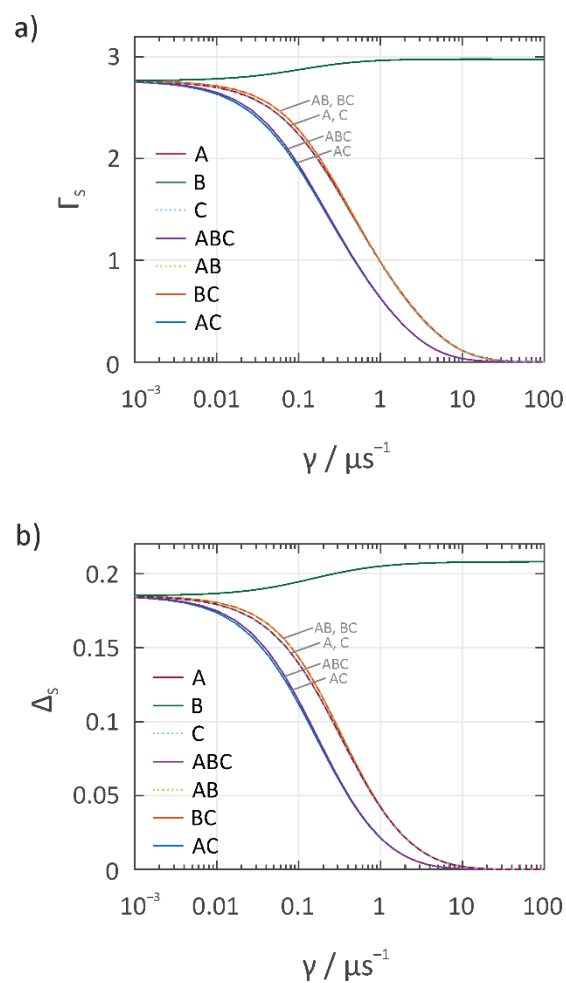


Figure S5: Dependence of Γ_s (a) and Δ_s (b) on the rate of random-field spin relaxation of the electron spins in various radicals of a model $[\text{FAD}^{\bullet-} \text{W}^{\bullet+}]$ radical pair subject to radical scavenging. Pertinent parameters: $\varphi = k_b/k_f = 1$; $B_0 = 50 \mu\text{T}$; $k_f = 0.1 \mu\text{s}^{-1}$; $k_c = 51.79 \mu\text{s}^{-1}$; $\text{A}^{\bullet-}$, $\text{B}^{\bullet+}$ and C^{\bullet} comprised N5 and N10 of $\text{FAD}^{\bullet-}$, N1 of $\text{W}_c^{\bullet+}$ and no magnetic nuclei, respectively.

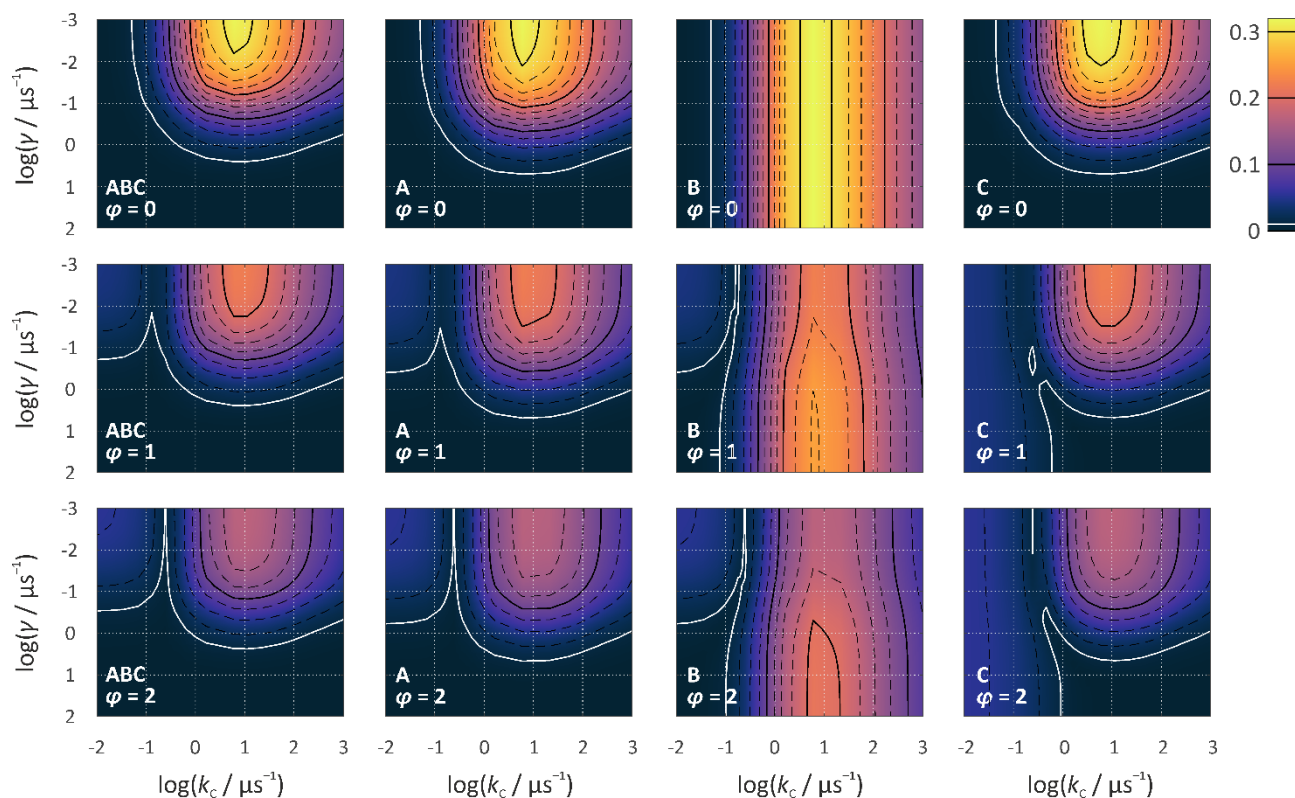


Figure S6: Contour plots of Δ_s as a function of k_c and γ for three different $\varphi = 0, 1,$ and 2 (rows) and random field relaxation in all three radicals (left) or either A, B, or C (right). The white and the (up to) three solid black contour lines corresponds to 1 %, 10%, 20% and 30%, respectively. The 1 % contour is used in the main text to discuss the resilience of the compass to spin relaxation. A^{*-}, B^{**} and C^{*} comprised N5 and N10 of FAD^{*-}, N1 of W_c^{**} and no magnetic nuclei, respectively. All simulation parameters were the same as for Figure 2 of the main manuscript.

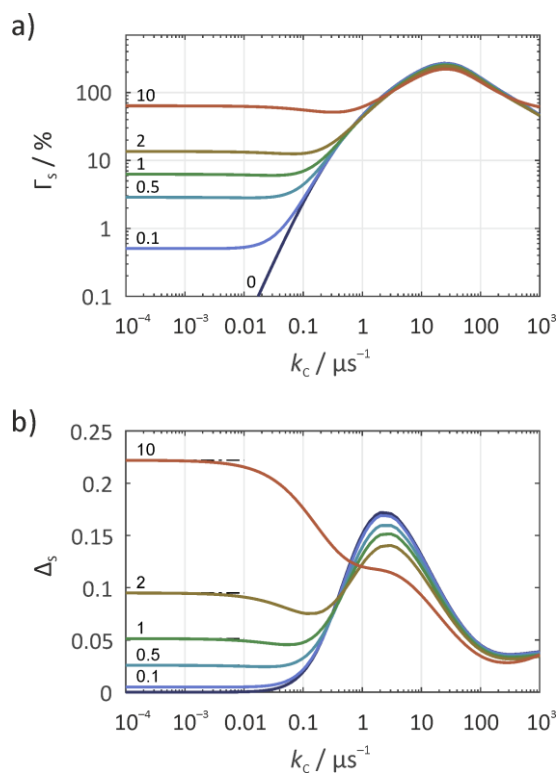


Figure S7: Anisotropic yields of the signalling state for a triplet-born $[\text{FAD}^{\bullet-} \text{Z}^{\bullet}]$ radical pair subject to radical scavenging. *a)* relative anisotropy (Γ_s), *b)* absolute anisotropy (Δ_s), both as a function of the scavenging rate constant, k_c , for various values of ϕ (indicated in the figure). The radical triad comprised N5, N10, H6, H8 (3 \times) and H β (2 \times) in $\text{FAD}^{\bullet-}$ and no hyperfine interactions in Z^{\bullet} or the scavenger. Comparison with calculations for the analogous singlet-born radical pair (see [1]) reveals that for $\phi = 0$, the anisotropy of the singlet states is independent of the initial spin multiplicity. Furthermore, for $\phi = 0$, the maximal $\Gamma_s = 2.7$ occurs at $k_c = 25.4 \mu\text{s}^{-1}$.

1. D. R. Kattnig and P. J. Hore, *Sci. Rep.*, 2017, **7**, 11640.

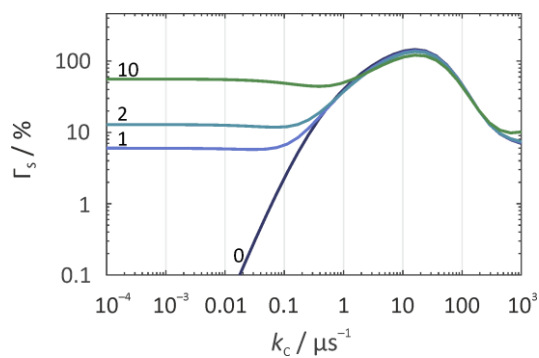


Figure S8: Relative anisotropy of the signalling state for a triplet-born [FADH[•] Z[•]] radical pair subject to radical scavenging. Γ_s is plotted as a function of the scavenging rate constant, k_c , for various values of ϕ (indicated in the figure). The radical triad comprised N5, N10 and H5 in FADH[•] and no hyperfine interactions in Z[•] or the scavenger. Hyperfine parameters have been taken from [2].

2. A. A. Lee, J. C. S. Lau, H. J. Hogben, T. Biskup, D. R. Kattnig and P. J. Hore, *J. R. Soc. Interface*, 2014, **11**, 20131063.